CALIBRATION CURVE OF SENSOR WORKING BY THE TRIANGULATION PRINCIPLE AND EFFECT OF TILT ON MEASUREMENT ABILITY

Lukáš HRIVNIAK[1]* – Michal ŠAŠALA[2] – Jozef SVETLIK[3] – Tomáš STEJSKAL[4]

[1] *Ing. Lukáš Hrivniak, Technical university of Košice, Letná 9/B, 042 00 Košice, Slovakia*

[2] *Ing. Michal Šašala, Technical university of Košice, Letná 9/B, 042 00 Košice, Slovakia*

[3] *prof. Ing. Jozef Svetlík, PhD. Technical university of Košice, Letná 9/B, 042 00 Košice, Slovakia*

[4] *Ing. Tomáš Stejskal, PhD. Technical university of Košice, Letná 9/B, 042 00 Košice, Slovakia*

*Corresponding author E-mail address: lukas.hrivniak@tuke.sk

Abstract

This paper deals with creating a calibration curve of a laser sensor that works on the principle of triangulation. It demonstrates the change of the calibration curve mainly by the different tilt angles of the sensor. The change in angle represents the effect of sensor mounting on the measurement results and the importance of taking proper mounting to obtain the most accurate measurement results. Calibration was performed under as stable ambient conditions as possible and using the optical standard as a suitable instrument for calibrating the sensors. The following article highlights the importance of calibration. The effect of sensor inclination on the calibration curve and the importance of correct sensor installation on measurement accuracy.

Keywords: Measurement, triangulation, calibration, calibration curve.

1 Introduction

Measuring instruments and measuring devices are currently subject to high precision requirements. It was necessary to develop measuring instruments and devices of such quality and precision that they could measure with sufficiently high accuracy. Therefore, the quality requirements of the measuring devices are now high. What ensures that a measuring device, measuring instrument or sensor works correctly, provided that the correct conditions of measurement and its use are met is calibration. Calibration can be expressed in various ways, such as data, calibration function, diagram, calibration curve or table [1]. This paper deals with the findings of the influence of the tilt sensor on its accuracy and repeatability. These were detected when calibrating the sensor. As a result of the calibration, a calibration curve was created at several sensor tilt angles, which show at first glance the changes in measurements at the different tilt angle of the triangulated sensor.

2 Meaning of the calibration curve

The operation of detecting and documenting data deviations that indicate a measuring instrument from a conventionally true value of a measured quantity is called calibration. The result of the calibration may be an indication, a calibration function, a calibration diagram, a calibration curve or a calibration table. However, the International Vocabulary of Basic and General Metrology Terms (VIM) does not define these terms in any detail or specifically describe the output documentation that arises during the calibration process [2]. Calibration should not be confused with the adjustment of the measuring system or with verification of the calibration. The calibration curve represents the relationship between the measurement sensor indication and the corresponding value of the measured quantity [3].

Each measuring instrument should be calibrated before placing it in normal operation or when the use of the measuring instrument has changed significantly. Furthermore, if the specified calibration time has elapsed, and also when the instrument starts to display inconsistent data [4]. The calibration interval may be shortened or extended for certain applications. If the sensor resp. the measuring device shows long-term stable results, the calibration interval can be extended. If there are any doubts about the correctness of the sensor data resp. of the measuring device, the sensor should first be checked for damage. If so, find the cause and then remove it. If not, the calibration interval should be halved [5, 6].

3 Description of measuring devices

Modern laser transducers based on the triangulated measurement principle are based on the fact that if the beam is reflected from the detected object at a constant angle, the distance of incident of the reflected beam on the front of the sensor is proportional to the distance of the detected object from the sensor. Nowadays there are many different standards. Their quality must be as high as possible. The most modern standards are currently optical standards. They are designed in different designs depending on how they are used in practice. Interferometer is an instrument designed for high precision measurements. [7]

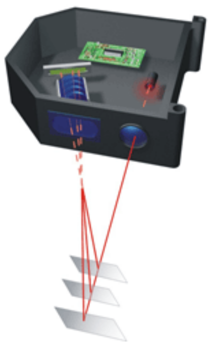

Fig. 1 *Diagram of the triangulated sensor*

Fig. 2 *Triangulation sensor optoNCDT 1420*

Its function is based on the principle of light interference. Advantages of the interferometer as well as the other mentioned standards are very high measuring accuracy, high speed and ability to measure angles. The interferometer is one of the most accurate and flexible systems currently used to calibrate transducers and measuring machines and instruments [8]. The Renishaw XL - 80 laser interferometer is shown in Fig. 2.

Fig. 3 *Laser head XL – 80*

Fig. 4 *Interferometer Renishaw*

4 Measuring by a sensor when changing the tilt angle

A very important factor in the measurement is to ensure the same conditions during the measurement as well as all repeated measurements. These relate not only to the measuring system itself but also to the environment in which the measurement takes place. It is the influence of the environment that has a considerable effect on the measurement and it is very difficult to ensure in particular temperature stability, which is very important during calibration [9, 10]. The measurements were carried out in a closed room under the same conditions. The conditions under which measurements were taken are shown in Table 1.

Table 1 *Measurement conditions*

Room air temperature	25 ° C
Atmospheric pressure	986 hPa
Air humidity	40 %
Number of people in the room	2
Cycle type	Linear
Measuring range	0 – 10 mm
Step size	0,5 mm
Angle adjustment accuracy	0,05 °
Powering the triangulating sensor	1,48 V / 0,03 A

For the purposes of measurement was assembled measuring assembly, which consisted of a sliding table on which the detected object was placed, measuring optics interferometer. For measurements on the measuring assembly, the triangulated transducer with holder was placed on a digital spirit level. Using it was tilted first by an angle of 0.20º and later by an angle of 0.60 º. The measurements result in calibration curves. They show the deviations of the values indicated by the triangulation sensor and the reference values represented by the laser interferometer. The measurement assembly is shown in Fig. 5 and Fig. 6.

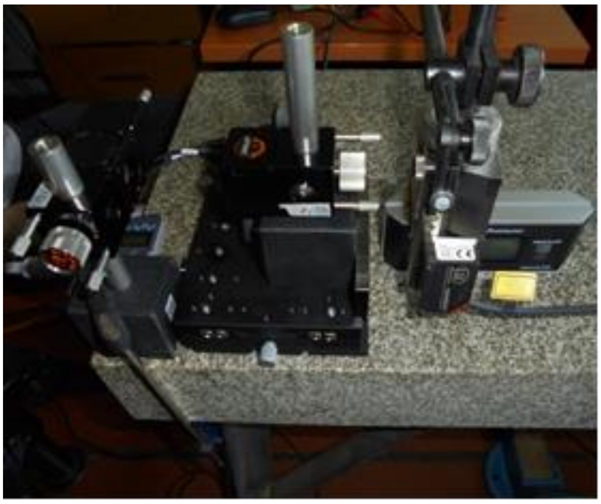

Fig. 5 *Measuring assembly*

Fig. 6 *Connection of the sensor optoNCDT 1420*

5 Measurement results and change of calibration curve

Using the prepared measuring set, a series of measurements were performed in order to detect deviations of the triangulation sensor from the measurement standard represented by a laser interferometer. After measurement, the values indicated by the triangulation sensor and the laser interferometer were entered in the table. Subsequently, they were subtracted from each other and the deviation values were determined [11, 12]. Using these values a calibration curve was created for the sensor without tilting respectively. with an angle of 0º. At the end of the last measurement, the sensor was mounted on a digital spirit level inclined at an angle of 20 ° and measurements were repeated. The same procedure was carried out at an angle of 40 ° and 60 °.

Measurements were repeated several times for each sensor position because of higher accuracy of the measured values. After processing all measurements, separate calibration curves were created for each sensor position measured. The graphs show that the graphs differ in these measurements due to the different tilt angle settings of the triangulation sensor. For the first measurements, the sensor was tilted by 0º, the calibration curve is shown in Fig. 7. In the second series of measurements it was an angle of 0.20º, the calibration curve is shown in Fig. 8. Subsequent measurements were made at an angle of 40 °, the calibration curve is shown in Fig. 9. The highest angle was 60º in the last series of measurements, the calibration curve is shown in Fig. 10.

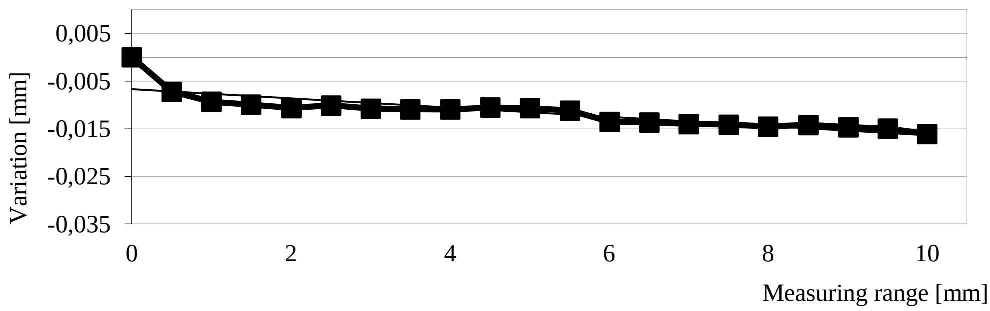

Fig. 7 *Calibration curve at 0º tilting*

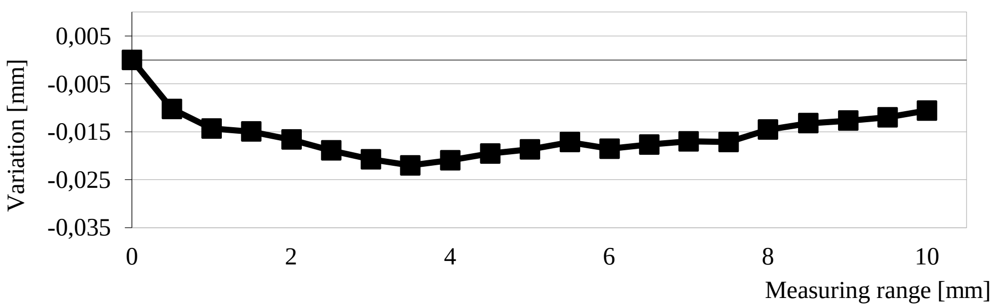

Fig. 8 *Calibration curve at 20º tilting*

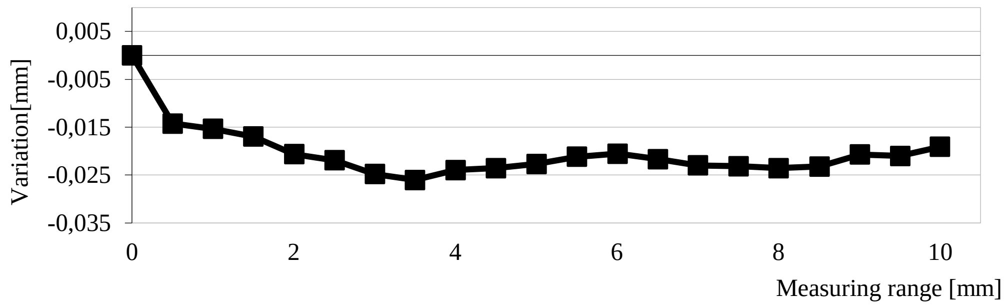

Fig. 9 *Calibration curve at 40° tilting*

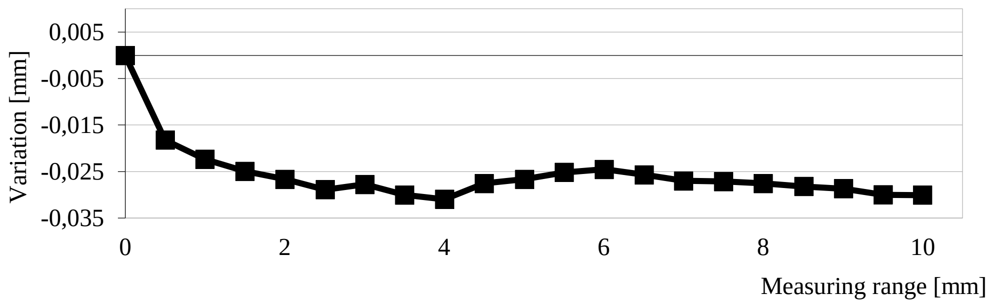

Fig. 10 *Calibration curve at 60° tilting*

A common graph of all measurements was created to compare the results and the differences in the calibration curves with the different tilt of the triangulation sensor. In this comparison, the difference in the calibration curves is clearly shown. The comparison shows the effect of tilting on the calibration curve. Gradually, as the tilt angle increases, the deviations of the triangulation sensor from the value represented by the standard and at the same time between the angles increase. As a result, the tri-regulating sensor is sensitive to adjustment. When using the sensor, this must be taken into account and quality mounting must be ensured. A comparison of the calibration curves of all series of measurements is shown in Fig. 11.

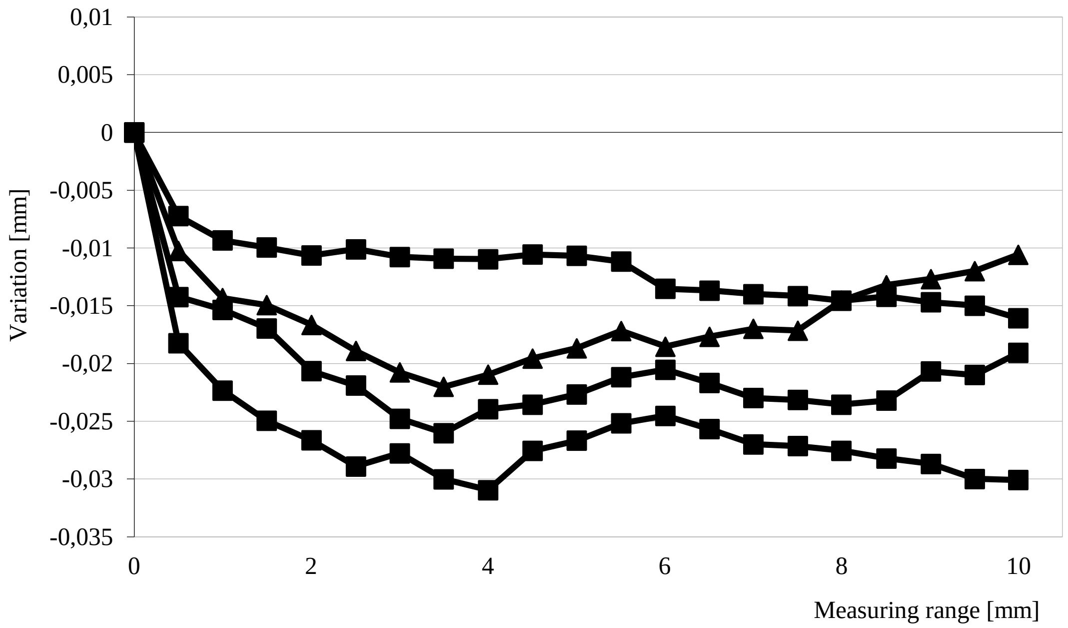

Fig. 11 *Changing the calibration curves*

6 Conclusion

Several series of measurements were performed, the purpose of which was to find out how the sensor working on the principle of triangulation will behave when changing the direction of the laser beam on the impact surface of the sensor. In this case, a change in the beam orientation is a change in the tilt angle of the entire sensor. The question was what effect this change would have on the accuracy and measuring ability of the sensor. The calibration curves show the deviations of the values indicated by the triangulation sensor and the reference values represented by the laser interferometer. The calibration curves were the same for each measurement. very similar. They only changed if the measurement conditions, such as the tilt angle of the sensor, have changed. This implies that the repeatability error is small compared to the measurement error. Conversely, the accuracy of the sensor varied over the entire measuring range. The calibration curve graph shows that at the beginning of the measuring range at a distance of 0 to 2 mm, the triangulation sensor measures with greater accuracy than for measurements in the range of 2 to 10 mm. Comparison of the calibration curves shows the effect of tilting on the calibration curve. This implies that the triangulated sensor is very sensitive to the angle at which it is mounted. When using the sensor, this must be taken into account and quality mounting must be taken into account, as this can directly affect the accuracy of the measured values.

Acknowledgements

This work was supported by the Slovak Research and Development Agency under the Contract no. APVV-18-0413 and APVV-15-0149.

References

[1] Kelemenová, T., Dovica, M.: Kalibrácia meradiel - 1. vyd. - Košice : TU - 2016. - 233 s.. - ISBN 978- 80-553-3069-3.

[2] Piteľ, J., Tóthová, M., Židek, K.: Technické meranie a diagnostika. Košice : TU, 2015. 117 s. ISBN 978-80-553-2016-8.

[3] Dobránsky, J., Panda, A., Manduľák, D.: Quality Monitoring in Production of the Parts in Automotive Industry. 1. vyd. - Ludenscheid : RAM-Verlag - 2015. - 190 p.. - ISBN 978-3-942303-36-1.

[4] Dobránsky, J., Baron, P., Kočiško, M., Telišková, M.: Monitoring diagnostic indicators during operation of a print machine. 2015. In: Advances in Science and Technology : Research Journal. Vol. 9, no. 28 (2015), p. 34-39. - ISSN 2299-8624.

[5] [22. 11. 2011] https://www.mmspektrum.com/clanek/kalibrace-a-presnost-mereni.html (cit. 22. 11. 2011)

[6] Baron, P., Kočiško, M., Dobránsky, J., Pollák, M., Telišková, M. Research and application of methods of technical diagnostics for the verification of the design node, 2016. In: Measurement. Vol. 94 (2016), p. 245-253. - ISSN 0263-2241

[7] MICRO-EPSILON : optoNCDT 1420 Instruction Manual [online]. 2008 [cit. 2019-01-15]. Dostupné z : https://www.contika.dk/wp-content/uploads/2018/03/NCDT-1420-manual.pdf

[8] Renishaw : Laser XL-80 manual [online]. 2011 [cit. 2011-12-14]. Dostupné z: http://www.renishaw.com/lasercalsupport/en/laser-calibration-systems-support-and-faq--11975.

[9] Škrabuľáková, E. F., Grešová, E.: Cost Saving via Graph Coloring Approach. In: Scientific Papers of the University of Pardubice : Series D. Roč. 27, č. 45 (2019). p. 152-160. ISSN 1211-555X.

[10] Pivarčiová, E., Božek, P., Domnina, K., Škultéty, Fedosov, S., Interferometric measurement of heat transfer above new generation foam concrete, In: Measurement Science Review, Volume 19, 2019, Issue 4, Pages 153- 160, DOI: 10.2478/msr-2019-0021.

[11] Skoog, Douglas A.; Holler, F. James; Crouch, Stanley R. (2007). Principles of Instrumental Analysis. Pacific Grove: Brooks Cole. p. 1039. ISBN 0-495-01201-7

[12] Faison, C. Douglas; Brickenkamp, Carroll S. (March 2004). "Calibration Laboratories: Technical Guide for Mechanical Measurements. NIST Handbook 150-2G. NIST.

WIND TURBINE IN GRID-OFF SYSTEM

Milan JUS

Ing. Milan Jus, PhD., Faculty of Special Technology, Alexander Dubček University of Trenčín, Pri Parku 19, 911 06 Trenčín, Slovakia
Corresponding author E-mail address: milan.jus@tnuni.sk

Abstract
The paper presents an analysis of a wind turbine, which is one of the sources of electricity in the Grid-Off system.

Keywords: wind turbine, Grid-Off system, electric generator, Photovolaic panel, wind conditions.

1 Introduction

The basic concept of a grid-off system consists of different sources that supply electricity. Mainly they are photovoltaic panels and wind turbine or even a diesel generator is still considered. This basic concept of grid-off system is shown in Fig. 1.

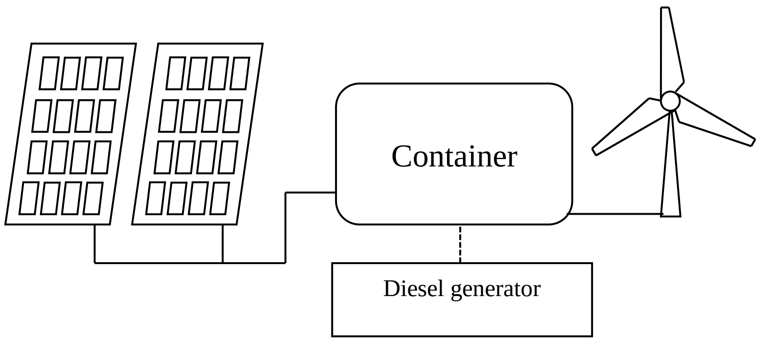

***Fig. 1** The basic concept of a Grid-Off system*

Another additional source is the thermoelegtric generator (TEG), which is based on the Seebeck effect. This TEG is part of photovoltaic panels. [1][2][3][4]

2 Wind power source

In this section, factors that affect wind turbine performance will be listed. The wind turbine performs a rotational movement based on the acting wind, which has kinetic energy E_k. The mathematical expression (1) is:

$$E_k = \frac{1}{2} m v^2 \tag{1}$$

where E_k is kinetic energy ($[E_k]$ = J), m is mass ($[m]$ = kg) and v is air speed $[v]$ = m/s.

In Fig. 2, the kinetic energy contained in the air element is located.

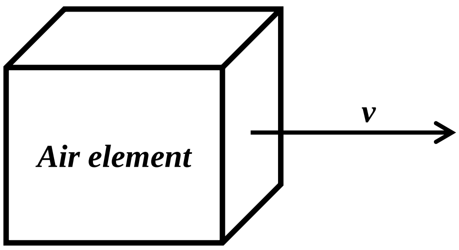

***Fig. 2** The kinetic energy contained in the air element with mass m*

Furthermore, we can express power P, which represents the energy per time (2). The mathematical expression is:

$$P = \frac{E_k}{t} = \frac{1}{2}\frac{m}{t} v^2 = \frac{1}{2} s v^2 \tag{2}$$

where s is mass flow ($[s]$ = kg/s).

Furthermore, it is possible to consider the wind time flow, which represents the flow of quantity over the area per unit of time, which is graphically shown in Fig. 3.

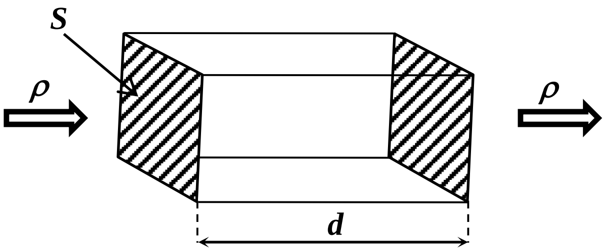

***Fig. 3** The wind time flow*

The mathematical expressed time flow of the wind will be

$$\frac{\rho}{t} = \frac{\frac{m}{V}}{t} = \frac{m}{Vt} = \frac{m}{Sdt} = \frac{1}{Sd}\frac{m}{t} = \frac{1}{Sd}s \tag{3}$$

where ρ is air density ($[\rho]$ = kg/m^3), wind time flow in volume $V = Sd$ ($[V]$ = m^3).

Next, from Equation (3) we express

$$s = \frac{\rho}{t}Sd = \rho S\frac{d}{t} = \rho Sv \tag{4}$$

If we substitute equation (4) into equation (2), we get

$$P = \frac{1}{2}sv^2 = \frac{1}{2}\rho Svv^2 = \frac{1}{2}\rho Sv^3 \tag{5}$$

In equation (5), the area S represents the area described by the wind turbine blades.

3 The maximum wind turbine power

Betz's law indicates the maximum power that can be extracted from the wind, independent of the design of a wind turbine in open flow. The law is derived from the principles of conservation of mass and momentum of the air stream flowing through an idealized "actuator disk" that extracts energy from the wind stream. [5]

In Fig. 4 is a schematic diagram of a constant density flow.

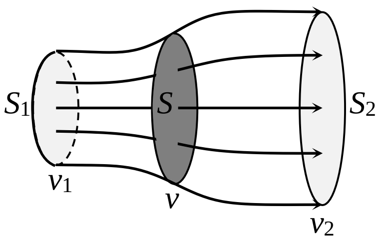

***Fig. 4** Schematic of fluid flow through a disk-shaped actuator*

Considering equation (4), for Fig. 4 can be expressed mathematically:

$$s = \rho S_1 v_1 = \rho Sv = \rho S_2 v_2 \tag{6}$$

where v_1 is the speed in the front of the rotor, v_2 is the speed downstream of the rotor, v is the speed at the fluid power device, ρ is the fluid density, the area of the turbine is given by S, and S_1 and S_2 are the areas of the fluid before and after reaching the turbine. [5-8]

The force exerted on the wind by the rotor is the mass of air multiplied by its acceleration. In terms of the density, surface area and velocities, this can be written as

$$F = m\frac{dv}{dt} = \frac{\overbrace{m}^{s}}{t}\Delta v = s\Delta v = \rho S v(v_1 - v_2) \tag{7}$$

The power (rate of work done) of the wind is

$$P = \frac{dE}{dt} = \frac{Fdx}{dt} = F\frac{\overbrace{dx}^{v}}{dt} = Fv = \rho S v^2(v_1 - v_2) \tag{8}$$

However, power can be computed another way, by using the kinetic energy. Applying the conservation of energy equation to the control volume yields

$$P = \frac{\Delta E}{\Delta t} = \frac{1}{2}s(v_1^2 - v_2^2) \tag{9}$$

Looking back at the continuity equation, a substitution for the mass flow rate yield

$$P = \frac{1}{2}\rho S v(v_1^2 - v_2^2) \tag{10}$$

If we compare equations (8) and (10), we get

$$\rho S v^2(v_1 - v_2) = \frac{1}{2}\rho S v(v_1^2 - v_2^2)$$
$$v(v_1 - v_2) = \frac{1}{2}(v_1^2 - v_2^2)$$
$$v(v_1 - v_2) = \frac{1}{2}(v_1 - v_2)(v_1 + v_2)$$
$$v = \frac{1}{2}(v_1 + v_2) \tag{11}$$

If we substitute equation (11) to (10) and then modify it, we get

$$P = \frac{1}{2}\rho S \overbrace{\frac{1}{2}(v_1 + v_2)}^{v}(v_1^2 - v_2^2) = \frac{1}{4}\rho S v_1^3\left(1 - \frac{v_2^2}{v_1^2} + \frac{v_2}{v_1} - \frac{v_2^3}{v_1^3}\right) \tag{12}$$

If we express the wind power before the turbine as

$$P_w = \frac{1}{2}\rho S v_1^3 \tag{13}$$

Then, the equation (12) can be adjusted to shape

$$P = \overbrace{\frac{1}{2}\rho S v_1^3}^{P_w}\overbrace{\frac{1}{2}\left(1 - \frac{v_2^2}{v_1^2} + \frac{v_2}{v_1} - \frac{v_2^3}{v_1^3}\right)}^{C_p} = C_p P_w \tag{14}$$

where

$$C_p = \frac{1}{2}\left(1 - \frac{v_2^2}{v_1^2} + \frac{v_2}{v_1} - \frac{v_2^3}{v_1^3}\right) = \frac{P}{P_w} \tag{15}$$

is dimensionless ratio of the extractable power P to the kinetic power P_w available in the undistributed stream.

Next we will look for the extreme coefficient C_p as a function of $\frac{v_2}{v_1}$, coefficient $C_p(\frac{v_2}{v_1})$ [9-12]

$$\left.\frac{dC_p}{d\xi}\right|_{\xi=\frac{v_2}{v_1}} = \frac{d}{d\xi}\left(\frac{1}{2}(1 - \xi^2 + \xi - \xi^3)\right) = 0 \tag{16}$$
$$\frac{1}{2}(-2\xi + 1 - 3\xi^2) = 0$$
$$-\frac{3}{2}\left(\frac{2\xi}{3} - \frac{1}{3} + \xi^2\right) = 0$$
$$\left(\xi - \frac{1}{3}\right)(\xi + 1) = 0 \tag{17}$$

The mathematical solution of equation (17) is the values of 1/3 and -1, while the real value of ξ=1/3 is real where the maximum value of C_p is reached is actually applicable:

$$C_p\Big|_{\frac{v_2}{v_1}=\frac{1}{3}} = \frac{1}{2}\left(1-\left(\frac{1}{3}\right)^2+\frac{1}{3}-\left(\frac{1}{3}\right)^3\right) = \frac{1}{2}\left(1-\frac{1}{9}+\frac{1}{3}-\frac{1}{27}\right) = \frac{1}{2}\frac{32}{27} = \frac{16}{27} \tag{18}$$

Then we can express equation (19) for the maximum value of C_p, which actually represents the maximum wind energy

$$P = \frac{16}{27}\frac{1}{2}\rho S v_1^3 = \frac{8}{27}\rho S v_1^3 \tag{19}$$

If we express it as a percentage, we are adding value

$$C_{p\ max} = \frac{16}{27} \cong 0.5926 = 59.26\ \% \tag{20}$$

4 Conclusion

The Grid-Off system is self-sufficient in terms of energy. In this paper, attention is paid to one power source, the wind turbine, as a power source for the Grid-Off system. Furthermore, the individual parameters are discussed, by means of which it is possible to maximize the output of the wind turbine, which is applicable either in the design of the turbine or only in the modification of the already used turbine. In theory, the maximum value we can get from wind energy is 59. 26 %.

Acknowledgements

The paper was treated within the project no. ITMS 26220220083 "Research technological base for designing applications for renewable energy in practice" EU operational program "Research and Development".

Európska únia
Európsky fond regionálneho rozvoja
Agentúra Ministerstva školstva, vedy, výskumu a športu SR pre štrukturálne fondy EÚ
Podporujeme výskumné aktivity na Slovensku
Projekt je spolufinancovaný zo zdrojov ES
Operačný program VÝSKUM a VÝVOJ

References

[1] Jus, M.: Využitie termoelektrického efektu v grid-off fotovoltických systémoch. In: Výzbroj a technika ozbrojených síl 2019 : 25. medzinárodná vedecká konferencia. - Liptovský Mikuláš : Akadémia ozbrojených síl generála Milana Rastislava Štefánika, 2019. - ISBN 978-80-8040-585-4. - s.83-88.
[2] Jus, M.: Thermoelectric generator model and simulation. In: Transfer 2019 : 20th International Scientific Conference. - Trenčín : TnUAD, 2019. - ISBN 978-80-8075-889-9. - s.71-78, CD ROM.
[3] Jus, M., Balla, J.: Parametric model of thermoelectric generator. In: University review. - ISSN 1339-5017. - Roč.13, č.3(2019), s.40-45.
[4] [02.03.2020], https://en.wikipedia.org/wiki/Thermoelectric_effect
[5] [02.03.2020], https://en.wikipedia.org/wiki/Betz%27s_law
[6] Ragheb, M., Ragheb, A. M.: Wind turbines theory—The Betz equation and optimal rotor tip speed ratio, fundamental and advanced topics in wind power. In R. Carriveau (ed.), Fundamental and Advanced Topics in Wind Power, InTech, 2011.
[7] [02.03.2020], https://www.fei.stuba.sk/buxus/docs/2019/AUTOREFERAT_Zuscak.pdf
[8] Zuščák, J., Janíček, F., Kijan, V., Váry, M.: Dynamic behavior of self-excited induction generator in Off-grid operation under resistive load. In Power engineering 2018. Control of Power Systems 2018 : 13th International scientific conference. Tatranské Matliare, Slovakia. June 5-7, 2018. 1. vyd. Bratislava : Slovak University of Technology, 2018, S. 89-94. ISBN 978-80-89983-00-1.
[9] Hansen, M.O.L.: Aerodynamics of Wind Turbines, 3rd ed., Routledge, 2015, ISBN 978-1138775077.
[10] Zuščák, J., Janíček, F.: Calculation of wind turbine power using Matlab. In ELITECH´16 [elektronický zdroj] : 18th Conference of doctoral students. Bratislava, Slovakia. June 8, 2016. 1. vyd. Bratislava : STU, 2016, CD-ROM, [5] s. ISBN 978-80-227-4561-1.
[11] [03.03.2020], https://en.wind-turbine-models.com/turbines/13-vestas-v47
[12] [03.03.2020], https://globalwindatlas.info/

MATHEMATICAL MODEL OF WIND TURBINE IN GRID-OFF SYSTEM

Milan JUS

Ing. Milan Jus, PhD., Faculty o Special Technology, Alexander Dubček University of Trenčín, Pri Parku 19, 911 06 Trenčín, Slovakia
Corresponding author E-mail address: milan.jus@tnuni.sk

Abstract
This paper deals with the construction of a mathematical model of a wind turbine, which is one of the sources in the Grid-Off system.

Keywords: mathematical model, wind turbine, Grid-Off system, electric generator, wind conditions.

1 Introduction

As one of the power sources of the Grid-Off system is a wind turbine. It is advantageous to work with a mathematical model for the need of experimental research. In Fig. 1 is a schematic connection of a wind turbine to a container, which is a Grid-Off system. [1-4]

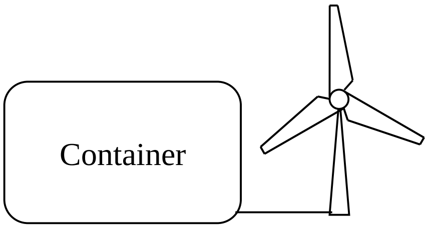

***Fig. 1** Wind turbine connection - Grid-Off system*

The process of producing electricity is, which in this case applies is as follows. The wind is carrying kinetic energy. Basically, the flow of air mass. The wind causes the propeller blades to rotate, so the kinetic energy is converted to mechanical energy. Subsequently, this mechanical energy is transformed into electrical energy by means of a suitable generator.

The mass flow energy passing through the area *S* determines the power of the intact air flow

$$P = \frac{1}{2}\rho S v^3 \tag{1}$$

where ρ is air density ($[\rho]$ = kg/m^3), *S* is area ($[S]$ = m^2) and *v* is velocity of flowing air ($[v]$ = m/s).

The mechanical energy that can be obtained by converting the kinetic energy of the air flow corresponds to the difference in power of the air flow upstream and downstream of the turbine, as shown in Fig. 2. The mathematical expression is as follows:

$$P = \frac{1}{2}\rho S_1 v_1^3 - \frac{1}{2}\rho S_2 v_2^3 \tag{2}$$

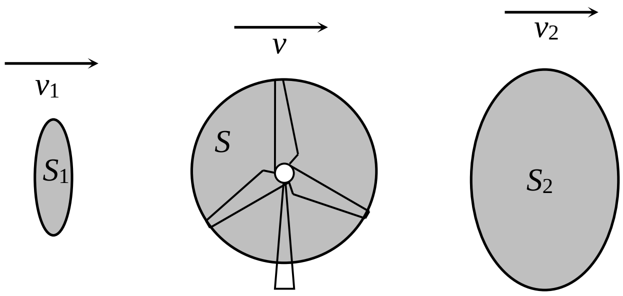

***Fig. 2** Air flow through turbine*

Based on the continuity equation is valid

$$\rho S_1 v_1 = \rho S_2 v_2 = \rho S_3 v_3 \tag{3}$$

We can then equation (2) using equation (3) shaped in the form

$$P = \frac{1}{2}\rho S_1 v_1 (v_1^2 - v_2^2) \tag{4}$$

The mechanical power of the wind turbine rotor can be expressed by relation (4) considering the momentum conservation law and its mathematical expression is

$$P = \frac{1}{4}\rho S v_1^3 \left(1 - \frac{v_2^2}{v_1^2} + \frac{v_2}{v_1} - \frac{v_2^3}{v_1^3}\right) = \underbrace{\frac{1}{2}\left(1 - \frac{v_2^2}{v_1^2} + \frac{v_2}{v_1} - \frac{v_2^3}{v_1^3}\right)}_{C_p} \underbrace{\frac{1}{2}\rho S v_1^3}_{P_w} \tag{5}$$

where C_p is dimensionless ratio of the extractable power P to the kinetic power P_w available in the undistributed stream. [4-5]

Maximum mechanical performance can only be achieved under certain conditions when the ratio v_2/v_1 is 1/3. In this case, the theoretical value of 59. 26 % is reached. [6]

The ratio of the peripheral speed of the rotor blade tip to the speed of the intact air flow upstream of the turbine is called turbine speed [7]

$$\lambda = \frac{\omega_r R_t}{v_1} \tag{6}$$

Next, we express the relation for the calculation of the mechanical moment T_m of the turbine rotor

$$T_m = \frac{P}{\omega_r} = \frac{C_p \frac{1}{2}\rho S v_1^3}{\omega_r} = \frac{1}{2}\rho S \frac{C_p v_1^3}{\frac{\lambda v_1}{R_t}} = \frac{1}{2}\rho S v_1^2 R_t \underbrace{\frac{C_p}{\lambda}}_{C_q} = \frac{1}{2}\rho S v_1^2 R_t C_q \tag{7}$$

where C_q is turbine rotor torque coefficient. [8-9]

2 Synchronous generator

The transformation of mechanical energy into electrical energy is carried out by means of a wind turbine, which is a synchronous generator with permanent magnets. The schematic diagram of the generator is shown in Fig. 3.

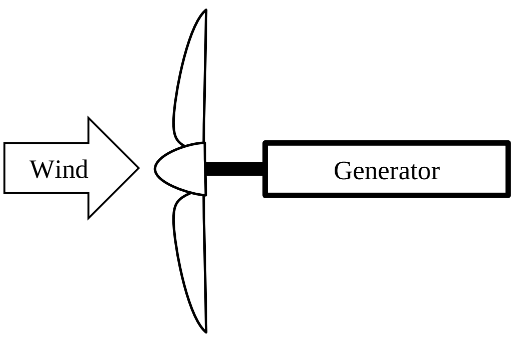

Fig. 3 *Transformation of mechanical energy into electrical energy*

The wind turbine includes blades that rotate the shaft on which the rotor of the permanent magnet synchronous generator is mounted. The rotor is formed by a permanent magnet, which causes a time-varying magnetic field, which results in voltage generation in the stator winding.

A schematic representation of a synchronous generator with a rotor of a permeable magnet and a stator formed by a winding is shown in Fig. 4.

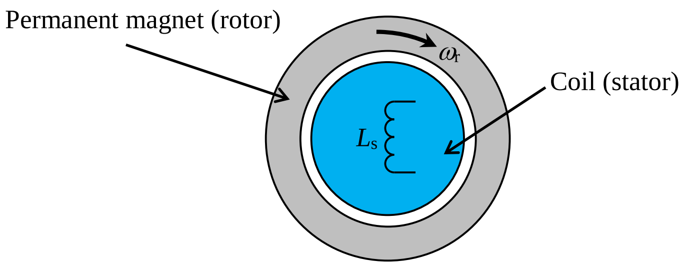

Fig. 4 *A schematic representation of a synchronous generator*

Depending on the torque balance condition, the dynamic system applies

$$T_m = T_g + J_a \frac{d\omega_r}{dt} \tag{8}$$

where T_m is the turbine torque produced by the wind on its blades, T_g is the braking torque of the generator with the load acting against the mechanical torque of the turbine and J_t is the moment of inertia of the aggregate. If we use the equation (7) and equation (8) we can adapt to the shape

$$\frac{d\omega_r}{dt} = \frac{T_m - T_g}{J_a} = \frac{\frac{1}{2}\rho S v_1^2 R_t C_q - T_g}{J_a} \tag{9}$$

The permanent magnets in the rotor, by their rotation around the stator, induce the internal voltage of the generator, for which

$$E_g = \mathrm{K}_{pm} \frac{\omega_r n_p}{2} \tag{10}$$

where K_{pm} is constant, which expresses the magnetic field strength of the permanent magnets of the generator, n_p is the number of poles of the generator and ω_r is the angular velocity of the rotor. [10-13]

If X is the reactance of the generator coil ($X = \omega_g L_s$, $\omega_g = n_p\omega_r/2$), and δ is angle between $\boldsymbol{U}_g$ and $\boldsymbol{E}_g$, the equation applies to the terminal voltage $\boldsymbol{U}_g$

$$\boldsymbol{U}_g = \boldsymbol{E}_g - \mathrm{j}X\boldsymbol{I}_g = |\boldsymbol{E}_g|\mathrm{e}^{j\delta} - X|\boldsymbol{I}_g|\mathrm{e}^{j\frac{\pi}{2}} = E_g\cos(\delta) + \underbrace{\mathrm{j}E_g\sin(\delta) - \mathrm{j}XI_g}_{0} = E_g\cos(\delta) \tag{11}$$

where

$$E_g \sin(\delta) = XI_g \tag{12}$$

The active power of the generator can be expressed as

$$P_g = \frac{3E_g U_g}{X}\sin(\delta) \tag{13}$$

Equation (13) using equation (11) and (10) can be modified to shape

$$P_g = \frac{3E_g E_g}{X}\underbrace{\cos(\delta)\sin(\delta)}_{\frac{1}{2}\sin(2\delta)} = \frac{3E_g^2}{2X}\sin(2\delta) = \frac{3\left(\mathrm{K}_{pm}\frac{\omega_r n_p}{2}\right)^2}{2X}\sin(2\delta) = \frac{3}{8X}\left(\mathrm{K}_{pm}\omega_r n_p\right)^2\sin(2\delta) \tag{14}$$

If we consider equation (12), then equation (14) can be expressed as

$$P_g = \frac{3E_g^2}{X}\cos(\delta)\sin(\delta) = \frac{3\left(\frac{XI_g}{\sin(\delta)}\right)^2}{X}\cos(\delta)\sin(\delta) = \frac{3I_g^2 X}{\tan(\delta)} \tag{15}$$

Generator moment T_g can be expressed depending on which equation we use, whether (15) or (14)

$$T_g = \frac{P_g}{\omega_r} = \frac{3I_g^2 X}{\omega_r \tan(\delta)} = \frac{3I_g^2 L_s n_p}{2\tan(\delta)} \tag{16}$$

$$T_g = \frac{P_g}{\omega_r} = \frac{3}{8X\omega_r}\left(K_{pm}\omega_r n_p\right)^2 \sin(2\delta) \qquad (17)$$

Based on these mathematical expressions, it is possible to construct a mathematical model by considering the particular parameters of a real wind turbine in the equations. The input parameter is the wind speed and the electrical output generated. It is also possible to add a connected load or use a more sophisticated wind model. Also in the model could be expressed regulation of wind turbine blades, possibly supplemented generator with speed control (angular speed).

3 Conclusion

In this paper is analyzed generator of electric energy, which is formed by wind turbine. It's about using that generator in the Grid-Off system. Mathematically, the continuity and continuity between the kinetic energy conversion that is contained in the wind and converted to the mechanical energy of the turbine are expressed. Subsequently, this mechanical energy is transformed into electrical energy by means of a synchronous permanent magnet generator.

Acknowledgements

The paper was treated within the project no. ITMS 26220220083 "Research technological base for designing applications for renewable energy in practice" EU operational program "Research and Development".

Európska únia
Európsky fond regionálneho rozvoja
Agentúra
Ministerstva školstva, vedy, výskumu a športu SR
pre štrukturálne fondy EÚ
Podporujeme výskumné aktivity na Slovensku
Projekt je spolufinancovaný zo zdrojov ES
Operačný program
VÝSKUM a VÝVOJ

References

[1] Jus, M.: Využitie termoelektrického efektu v grid-off fotovoltických systémoch. In: Výzbroj a technika ozbrojených síl 2019 : 25. medzinárodná vedecká konferencia. - Liptovský Mikuláš : Akadémia ozbrojených síl generála Milana Rastislava Štefánika, 2019. - ISBN 978-80-8040-585-4. - s.83-88.

[2] Jus, M.: Thermoelectric generator model and simulation. In: Transfer 2019 : 20th International Scientific Conference. - Trenčín : TnUAD, 2019. - ISBN 978-80-8075-889-9. - s.71-78, CD ROM.

[3] Jus, M., Balla, J.: Parametric model of thermoelectric generator. In: University review. - ISSN 1339-5017. - Roč.13, č.3(2019), s.40-45.

[4] [02.03.2020], https://en.wikipedia.org/wiki/Betz%27s_law

[5] Ragheb, M., Ragheb, A. M.: Wind turbines theory—The Betz equation and optimal rotor tip speed ratio, fundamental and advanced topics in wind power. In R. Carriveau (ed.), Fundamental and Advanced Topics in Wind Power, InTech, 2011.

[6] Zuščák, J., Janíček, F., Kijan, V., Váry, M.: Dynamic behavior of self-excited induction generator in Off-grid operation under resistive load. In Power engineering 2018. Control of Power Systems 2018 : 13th International scientific conference. Tatranské Matliare, Slovakia. June 5-7, 2018. 1. vyd. Bratislava : Slovak University of Technology, 2018, S. 89-94. ISBN 978-80-89983-00-1.

[7] Hau, E.: Wind Turbines: Fundamentals, Technologies, Application, Economics. 2nd. Edition. Berlin: Springer, 2006. ISBN 3-540-24240-6.

[8] Hansen, M.O.L.: Aerodynamics of Wind Turbines, 3rd ed., Routledge, 2015, ISBN 978-1138775077.

[9] Zuščák, J., Janíček, F.: Calculation of wind turbine power using Matlab. In ELITECH´16 [elektronický zdroj] : 18th Conference of doctoral students. Bratislava, Slovakia. June 8, 2016. 1. vyd. Bratislava : STU, 2016, CD-ROM, [5] s. ISBN 978-80-227-4561-1.

[10] Mellah, H., Hemsas, K. E.: Simulations Analysis with Comparative Study of a PMSG Performances for Small WT Application by FEM International Journal of Energy Engineering e-ISSN: 2163-1905. [Online]. 2015, [cit. 03.03.2020]. Dostupné na: http://article.sapub.org/10.5923.j.ijee.20130302.03.html

[11] [03.03.2020], https://www.vutbr.cz/www_base/zav_prace_soubor_verejne.php?file_id=99990

[12] Heier, S.: Grid Integration of Wind Energy. 3rd. Edition. John Wiley & Sons Ltd., 2014. ISBN 978-1-119-96294-6.

[13] Schaffarczyk, A.P.: Introduction to Wind Turbine Aerodynamics. Berlin: Springer, 2014. ISBN 978-3-642-36408-2.

SIMULATION OF A MATHEMATICAL MODEL OF A WIND TURBINE

Milan JUS

Ing. Milan Jus, PhD., Faculty of Special Technology, Alexander Dubček University of Trenčín, Pri Parku 19, 911 06 Trenčín, Slovakia
Corresponding author E-mail address: milan.jus@tnuni.sk

Abstract
This paper presents a mathematical model of a wind turbine and its simulation. This is one of the main resources available to the island system (Grid-Off system).

Keywords: wind turbine, island system, Grid-Off system, renewable energy source.

1 Introduction to wind turbine

A wind turbine is basically a converter, or in other words a device that transforms one type of energy into another. In this case, it is the transformation of mechanical energy into electrical energy.

The source of mechanical energy is the flow (flow) of air, which acts on the turbine blades. The blades are located on a shaft which is coupled to a permanent magnet (magnet). The magnets are a rotating part, which is named the rotor. The stator consists of a coil (coils) of wound copper conductor. Due to the changing magnetic field (PM - permanent magnets), an electrical voltage is induced at the terminals (terminals) of the coil / coils. In essence, it is a synchronous generator, since the variable electric field is coupled (synchronized) with the speed of the changing and magnetic fields. [1-5]

A schematic block diagram of a wind turbine as a synchronous generator is shown in Fig. 1.

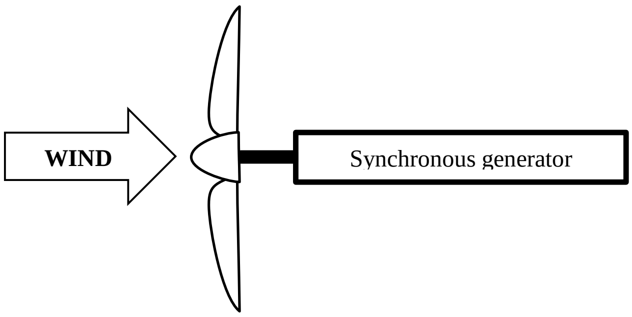

Fig. 1 *Principle block diagram of a wind turbine*

The kinetic energy of wind (air) is converted into mechanical energy of a rotating shaft. However, the validity of the continuity implies that the flow rate slows down on the turbine, since the air flow in front of the blades is intact with the velocity v and behind the blades the flow velocity is different. This fact is expressed by the power coefficient of the turbine C_p, which expresses the ratio of the mechanical power of the turbine P_m to the power of the intact air flow P_0, which is expressed by equation (1)

$$C_p = \frac{P_m}{P_0} \tag{1}$$

The maximum value of the turbine power coefficient is 0.59259, while physically feasible turbines have smaller values. [5-10]

We calculate the mechanical moment by the ratio of the mechanical power of the turbine to the angular velocity of the rotor ω_r, which we express mathematically as equation (2)

$$T_m = \frac{P_m}{\omega_r} = \frac{C_p \frac{1}{2}\rho A_r v^3}{\omega_r} = \frac{1}{2}\rho v^3 \frac{C_p A_r}{\omega_r} \tag{2}$$

where ρ is the air density and A_r is the rotor area. [11-12]

The mechanical connection of the wind turbine is such that if we proceed chronologically, the blades (blades) of the wind turbine are connected to the shaft to which the generator rotor is further connected. The blades generate a mechanical moment T_m. The shaft itself has a certain distributed weight, which is expressed by the moment of inertia, which depends on the time change of the angular velocity of the rotor. In terms of direction, the torque of the generator T_g (braking torque) acts in the opposite way, the mathematical expression of the balance of moments is represented by equation (3)

$$T_m = J_a \frac{d\omega_r}{dt} + T_g \tag{3}$$

From the point of view of creating a mathematical model, it is necessary to modify equation (3) into the form (4)

$$\frac{d\omega_r}{dt} = \frac{1}{J_a}\left(T_m - T_g\right) \tag{4}$$

Next we need to calculate the torque of the generator, which is expressed as (5)

$$T_g = \frac{3 I_g^2 L_s n_p}{2 \tan(\delta)} \tag{5}$$

where I_g is the current flowing through the generator load, L_s is the stator inductance, n_p is the number of generator poles and the angle δ is between the internal generated voltage E_g and the voltage at the generator terminals U_g.

The internal voltage of the E_g generator depends on the force of the permanent magnet k_{PM}, the angular velocity of the rotor ω_r and the number of poles n_p, which is mathematically expressed as equation (6)

$$E_g = k_{PM}\omega_r \frac{n_p}{2} \tag{6}$$

If we connect the load R_z to the terminals of the generator, which is schematically shown in Fig. 2, we can express the equation for the generated voltage U_g at the terminals as equation (7) and the current I_g passing through the load as equation (8)

$$U_g = E_g \cos(\delta)\cos\left(\omega_g t\right) \tag{7}$$

$$I_g = \frac{U_g}{R_z} = \frac{E_g \cos(\delta)}{R_z}\cos\left(\omega_g t\right) \tag{8}$$

where ω_g is the angular frequency of the generator current.

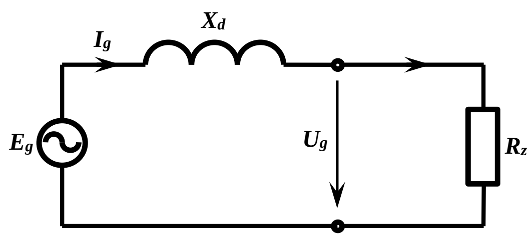

Fig. 2 *Connecting the load to the generator*

2 Mathematical model of wind turbine and its simulation

Based on the mathematical expressions in the previous section, a mathematical model will be constructed, which essentially consists of four basic blocks as shown in Fig. 3.

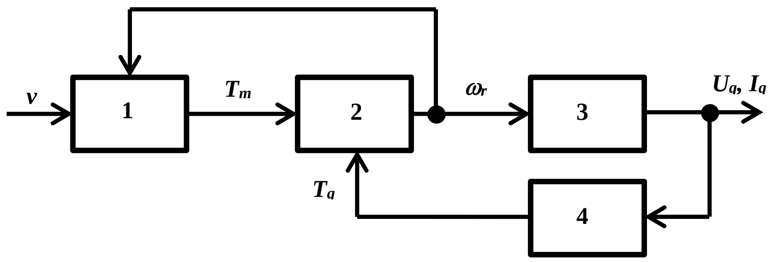

Fig. 3 *Block diagram of a mathematical model of a wind turbine*

The compilation of the model and its simulation was carried out in the SCILAB software, specifically in the XCos part, where individual blocks 1 to 4 as whole units (sub-blocks) were created and they contained individual blocks / parts of the scheme that expressed mathematical implementation as required, which is described in the following text.

Block 1 represents the incorporation of equation (2) into the model, where the inputs are the wind speed and the value of the angular velocity of the rotor. There are also constants in the model, which are summarized in Tab. 1. The model of block 1 is shown in Fig. 4.

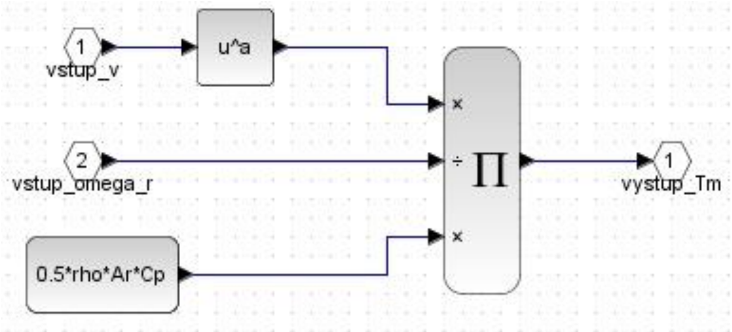

Fig. 4 *Block diagram of block 1 - the output is the mechanical torque* T_m

Block 2 after the adjustment expresses equation (4), the adjustment is necessary because the equation expresses the time change, where the inputs are the mechanical torque (output from block 1) and the generator torque, which is the output of block 4. The block diagram of block 2 is in Fig. 5.

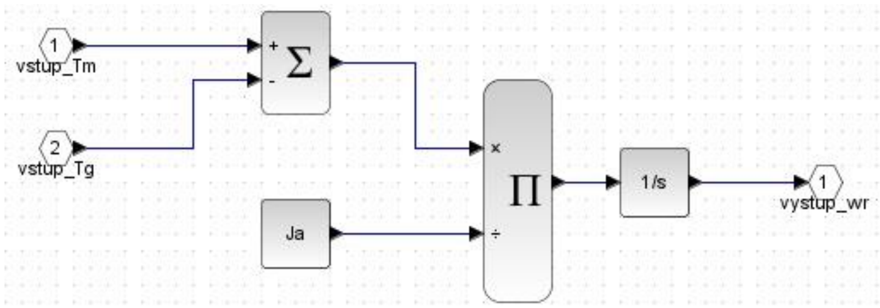

Fig. 5 *Block diagram of block 2 - the output is the angular speed of the rotor* ω_r

Block 3 includes equations (6), (7) and (8) and its output is the electrical quantities U_g and I_g. The block diagram that implements this is shown in Fig. 6.

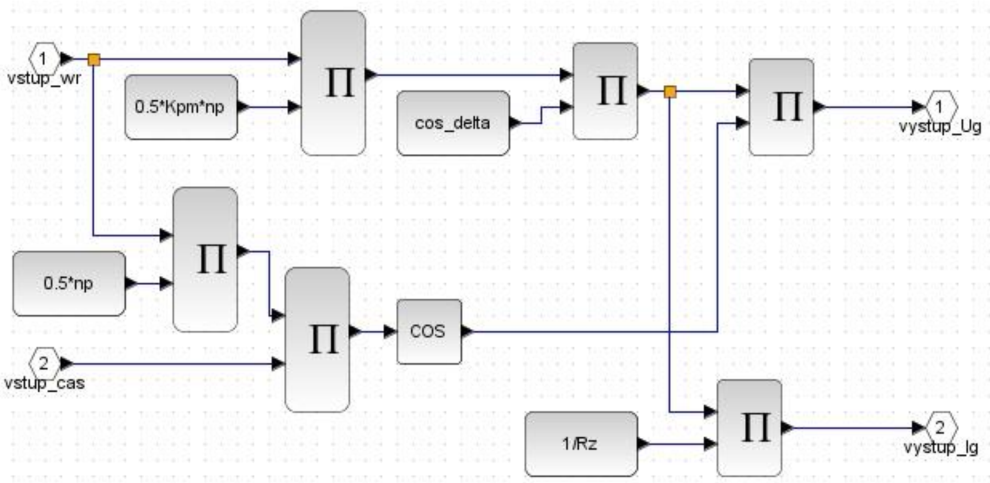

Fig. 6 *Block diagram of block 3 - the output are electrical quantities* U_g *and* I_g

Block 4 uses as input only the current flowing through the load I_g and the output is the torque of the generator, it is basically the realization of equation (5). The block diagram implementing Equation (5) is shown in Fig. 7.

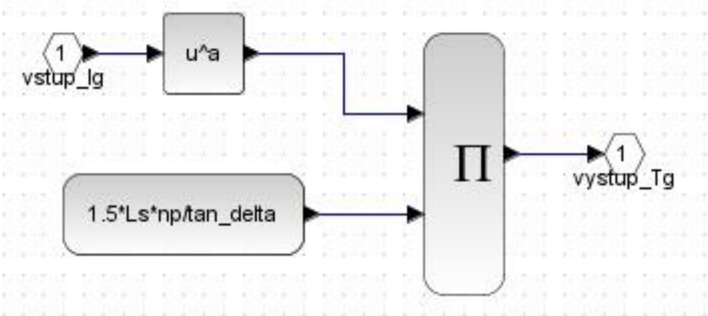

Fig. 7 *Block diagram of block 4 - the output is the torque of the generator T_g*

There were also constants in the individual parts of the model that need to be initialized at the beginning of the simulation. The specific values of the constants used are given in the following Table 1.

Table 1 *Stated values of constants used in the wind turbine model*

The name of the constant	*Value*	*Comment*
Kpm	10.3668 V.s	force PM
np	10	number of generator poles
delta	0.1745329 rad	angle between E_g and U_g
cos_delta	0.9848078	cosine angle delta
tan_delta	0.1763270	sine angle delta
Ls	3.07e-3 H	stator inductance
Ja	0.748 kg.m^2	the resulting moment of inertia
rho	1.29 kg.m^{-3}	air density
Rt	1.35 m	rotor radius
Ar	5.7255526 m^2	rotor surface
Cp	0.5	power factor
Rz	100 Ω	load resistance

The resulting block diagram represents the circuit according to Fig. 3, where the individual blocks are interconnected and also blocks for displaying waveforms are added. Such a complete connection of the wind turbine model is shown in Fig. 8.

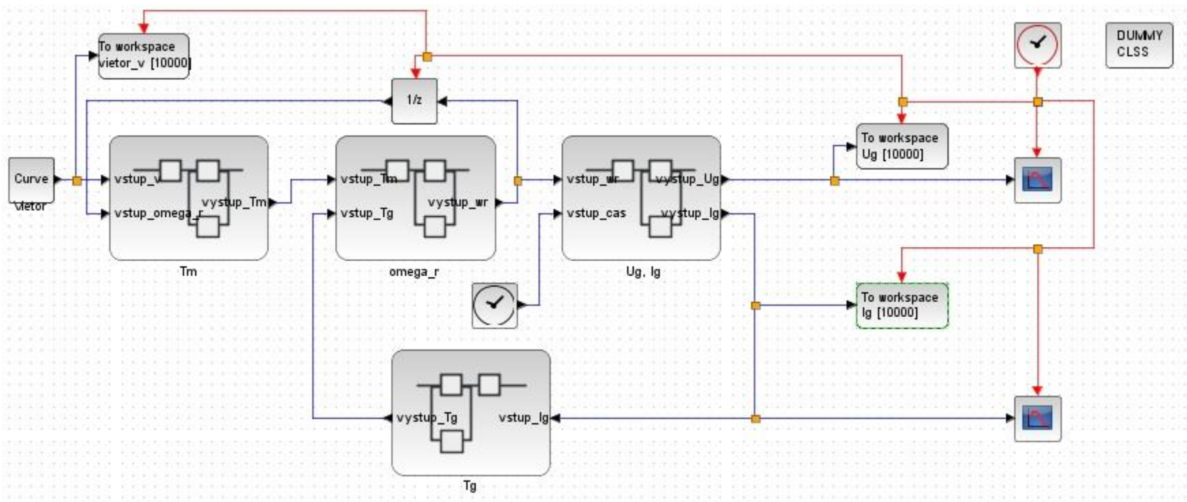

Fig. 8 *Final simulation model of a wind turbine*

In the given model shown in Fig. 8, a simulation was performed where the input to the model was a variable wind speed to which the wind turbine is exposed. The end load was a resistance with a value of 100 Ω and only the course of the generated current I_g passing through the load R_z was evaluated.

In Fig. 9 shows the simulated course of the generated current at the same time as the course expressing the change in wind speed (shown in blue), where it is possible to see the reaction to the change in current (shown in green) size from the change in wind speed. The value of wind speed is in $m.s^{-1}$ and the value of current magnitude in A, since these values are close in size, therefore one scale on the y-axis is used.

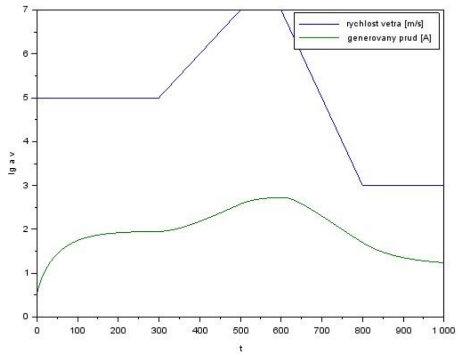

Fig. 9 *The simulated course of the generated Ig current*

3 Conclusion

In this paper, a mathematical model designed to simulate a wind turbine was designed and built. The current generated through the load was mainly simulated and presented. The input to the simulation was the variable magnitude of the wind speed acting on the wind turbine. The simulation shows that if we take I_{gmax} = 2.7 A and a load of 100 Ω, the maximum power was 730 W.

Acknowledgements

The paper was treated within the project no. ITMS 26220220083 "Research technological base for designing applications for renewable energy in practice" EU operational program "Research and Development".

Európska únia
Európsky fond regionálneho rozvoja
Agentúra Ministerstva školstva, vedy, výskumu a športu SR pre štrukturálne fondy EÚ
Podporujeme výskumné aktivity na Slovensku
Projekt je spolufinancovaný zo zdrojov ES
Operačný program VÝSKUM a VÝVOJ

References

[1] [16.03.2020], https://en.wikipedia.org/wiki/Betz%27s_law

[2] Ragheb, M., Ragheb, A. M.: Wind turbines theory—The Betz equation and optimal rotor tip speed ratio, fundamental and advanced topics in wind power. In R. Carriveau (ed.), Fundamental and Advanced Topics in Wind Power, InTech, 2011.

[3] Zuščák, J., Janíček, F., Kijan, V., Váry, M.: Dynamic behavior of self-excited induction generator in Off-grid operation under resistive load. In Power engineering 2018. Control of Power Systems 2018 : 13th International scientific conference. Tatranské Matliare, Slovakia. June 5-7, 2018. 1. vyd. Bratislava : Slovak University of Technology, 2018, S. 89-94. ISBN 978-80-89983-00-1.

[4] Hansen, M.O.L.: Aerodynamics of Wind Turbines, 3rd ed., Routledge, 2015, ISBN 978-1138775077.

[5] Zuščák, J., Janíček, F.: Calculation of wind turbine power using Matlab. In ELITECH´16 [elektronický zdroj] : 18th Conference of doctoral students. Bratislava, Slovakia. June 8, 2016. 1. vyd. Bratislava : STU, 2016, CD-ROM, [5] s. ISBN 978-80-227-4561-1.

[6] [18.03.2020], https://globalwindatlas.info/

[7] [18.03.2020], https://en.wind-turbine-models.com/turbines/13-vestas-v47

[8] Hau, E.: Wind Turbines: Fundamentals, Technologies, Application, Economics. 2nd. Edition. Berlin: Springer, 2006. ISBN 3-540-24240-6.

[9] Mellah, H., Hemsas, K. E.: Simulations Analysis with Comparative Study of a PMSG Performances for Small WT Application by FEM International Journal of Energy Engineering e-ISSN: 2163-1905. [Online]. 2015, [cit. 19.03.2020]. Dostupné na: http://article.sapub.org/10.5923.j.ijee.20130302.03.html

[10] Schaffarczyk, A.P.: Introduction to Wind Turbine Aerodynamics. Berlin: Springer, 2014. ISBN 978-3-642-36408-2.

[11] Heier, S.: Grid Integration of Wind Energy. 3rd. Edition. John Wiley & Sons Ltd., 2014. ISBN 978-1-119-96294-6.

[12] [20.03.2020], https://www.scilab.org/use-cases/model-reduction-for-wind-farm-optimization

RENEWABLE ENERGY SOURCES IN THE CASE OF CRISIS SITUATIONS

Peter LIPTÁK[1]* – Ivan KOPECKÝ[2]

[1] *Peter Lipták, Faculty of Special Technology, Alexander Dubček University of Trenčín, Pri parku 19, 911 06 Trenčín. Slovak Republic.*

[2] *Ivan Kopecký, Faculty of Special Technology, Alexander Dubček University of Trenčín, Pri parku 19, 911 06 Trenčín. Slovak Republic*

*Corresponding author E-mail address: peter.liptak@tnuni.sk

Abstract

Operation of special equipment is possible in crisis situations. It is because special equipment is designed for operation in non-standard often extreme conditions and situation, it is available, it has a high degree of crossing capability and it is able to provide basic living conditions even in field, e.g. provision of power for hospital, transportation of wounded and injured persons, supplies, medical care in field conditions, delivery of potable and utility water etc. The authors in the paper deal with a possibility to provide electric energy through advanced renewable sources, especially in meeting tasks in areas with no public mains, possible supplies of potable and non-potable water, embedding such assets into mobile systems. The authors in publication summarize results of research within the „Use of renewable sources of energy in practice“project. System of modeling and computer-aided simulation of renewable sources of energy has been proposed within this project. Application of a system for designing of power systems in logistic containers is expected. The knowledge on power balance of logistic containers operated by the SR Armed Forces in missions abroad is summarized in the last chapter of the paper.

Keywords: Crisis situations, renewable sources of energy, photovoltaic collectors, logistic container, power systems, mobile assets of crisis management

1 Introduction

To provide basic human needs in solving crisis situation there is a need to provide an affected area with energy and water. The authors within a research program have been solving such provision assuming that equipment will be deployed in different environs and will use energy from solar radiation and wind energy as well in addition to standard initial energy and power supply. Mobile solution has been proposed, namely embedding the equipment and devices into containers that are transportable to a destination by a rotor-wing by a truck or a vessel. One of the prepositions for a possible commissioning of the equipment is a presumption of a machine quality and its reliability, equipment within limits of operational parameters. In operational practice of special equipment, e.g. machines and equipment (engineer equipment) the repairmen and operators challenged a task to create conditions to use some selected equipment, e.g. electric devices and appliances in critical situations as well, e.g. in humanitarian relief, , in military and peace observation missions of international organizations or within international exercises. With regard to a fact, that nearly always in such situations machines and equipment is to be deployed, including electric machines, the experience in this area was generalized as a background aiming to start a technical preparation for next missions and their logistic support.

2 Materials and methods

Under a „CRISIS SITUATION“notion for purposes of this paper we understand an unplanned, specific situation resulting in:

- Threat to persons, environment, property in a larger scale.
- Presumptions for a rise of such situation can be determined only with a low probability.
- The situation occurs resulted from an unpredictable environmental situation (e.g. disasters and casualties, earthquakes, floods etc.), from unpredictable activity of persons (e.g. terrorist attacks etc.), unthinkable crashes of systems and facilities, (e.g. nuclear power plant accident resulting from disasters etc.), and other unpredictable situations.

From a point of view of providing a solution for such situation there is a need to be ready for such solution in terms of being equipped with appropriate equipment, material, and assets. The authors of the paper deal with a special equipment under their purview.

Quality and operational reliability are the basic requirements laid on special equipment. Under quality and operational reliability notion for this paper we are considering quality of a whole technological cycle, quality of a machine and facility as a whole.

In literature an operational reliability (or service dependability) notion is characterized as a feature of a product enabling meeting specified functions within the permitted tolerance under given operating conditions and in a requested operating period [1]. Service dependability of a product, facility, and machine in particular contains ability:

- To work permanently within the permitted tolerance of required parameters,
- To keep a repair ability (to retain a possibility to remove failures),
- To withstand a short-term overloading (resistance of the product),
- To work for a certain period even with small damages, i.e. with worsened operating parameters (product´s viability),
- Maintenance undemandingness and its small range (maintenance friendliness and efficiency).

From a user point of view the reliability is perceived as an integral set of technical, qualitative, economical, ergonomic and other properties of a product, influencing its total technical life [2]. Within reliability theory we differentiate:

- properties,
- reviewed areas and their basic characteristics,
- phenomena, conditions and activities,
- variable working values,
- failures,
- indicators of reliability,
- Indicators of a failure-free operation
- life-cycle indicators,
- indicators of storage stability
- indicators of maintainability
- complex indicators
- testing,
- backup.

As extreme conditions are considered all conditions, that are beside values being typical for Central European temperate climate zone, Tab.1.

***Table 1** Characteristics of a temperate climate zone*

The lowest temperature of air	-40°C
The highest temperature of air	+40°C
The highest relative humidity	95%
The highest absolute humidity	60 g.m^{-3}
The highest intensity of solar radiation	1120 W.m^{-2}
The highest intensity of thermal radiation	600 W.m^{-2}
The highest speed of air	20 m.s^{-1}

***Table 1** Table Caption*

No	**Pressure [MPa]**	**Processing conditions**
1a	400	debinding
1b	600	debinding
2a	400	debinding, ECAP-BP
2b	600	debinding, ECAP-BP
3a	400	debinding, sintering, ECAP-BP
3b	600	debinding, sintering, ECAP-BP
4	100	annealing
5	0	hardening

Area, in which the selected equipment and machines were reviewed, is characterized as environs with increased corrosion aggressiveness, dusty environment with nonflammable dust, however the one deteriorating dielectric permittivity and electric piercing strength due to its conductivity, environment with quakes and environment with biological vermin.

Various types of simulation chambers are used when simulating the effects of environment on parts and devices. Inside these chambers there is such simulating environment established, where the product application is supposed to be, e.g.:

- Humid heat trial – cyclical mode
- Humid heat trial – acyclic mode
- Mildew trial
- Air-tightness trial
- Solar radiation trial

- Atmospheric pressure trial
- Temperature alternation trial, frost trial
- dry heat trial
- salt-haze trial
- low pressure trial
- dust trial.

In case when equipment is deployed in conditions with an increased concentration of air pollutants in long-shore areas we recommended the following tests:

- corrosion test in a condensation chamber – to verify resistance of materials and surface protection, when it relates an effect by an increased humidity or an increased concentration of SO_2 with no other effecting factors,
- corrosion test in a salt haze – verifies material resistance and surface protection in long-shore atmosphere with a decisive factor – a sea water aerosol,
- solar radiation trial– verifies the product resistance to light and thermal effects of solar radiation,
- dust and sand trial – simulation of desert conditions,
- dry and wet heat test,
- mildew trial – simulation of material having been biologically invaded,
- vibration trial.

These trials has been proved by a next operation of equipment and material in practice, e.g. in areas of equatorial Africa and on Cyprus Island. As we monitored the renovated objects, we chose the failure and renovation flows as reliability criteria. Properties of renovated objects are expressed by $\mathrm{H}(t)$ value, a mean number of failures of a renovated object for t period:

$$\mathrm{H}(t) = \frac{1}{N}\sum_{i=1}^{N} n_i(t) \tag{1}$$

where $n_i(t)$ is a number of failures of the i-th renovated object during t operating period, N is a number of objects being reviewed. From statistics point of view, a failure flow characteristics is appropriate, that we expect in a short time period Δt. This characteristic is expressed by a relation:

$$\hat{h}(t) = \frac{\Delta \mathrm{H}(t)}{\Delta t} = \frac{\sum_{i=1}^{N}\left[n_i(t+\Delta t) - n_i(t)\right]}{N.\Delta t} \tag{2}$$

where $\Delta \mathrm{H}(t)$ is an increase of an average number of failures for a short time interval Δt, or an average number of failures in a time interval (t,t+Δt). Due to statistical assessment of a real number of failures during year operating period, it was possible to consider, that the failures of a renovated object are ruled by an exponential rule of distribution with a λ failure intensity. In a particular situation, Tab.3, was a value of a mean number of failures of a renovated object for 1 operating year (tests were made 1 month after completion of a rain season) a number from interval (0, 1 – 0, 4) in a so called stable state of reliability (test run was made before exporting abroad, in ageing state we do not recommend to operate an equipment abroad).

Coefficient of technical usage:

$$K_{tv} = T/\left(T + T_p + T_o\right) \tag{3}$$

is a readiness coefficient:

$$K_p = T/\left(T + T_o\right) \tag{4}$$

where T is an average period between failures of a renovated object, T_p is an average period of a shut-down, T_o is an average repair period. From a view of a possible increase of machine and equipment reliability, being operated in climate conditions we have chosen a backing up method. Backup is one of basic methods in improving reliability of machines and equipment. This relation is applied for parallel arrangement of elements (Fig.1):

$$R_p(t)=1-\prod_{i=1}^{k}1-\exp\left[-\left(\frac{t}{a_i}\right)^{b_i}\right]=1-\prod_{i=1}^{k}F_i(t) \qquad (4)$$

where $R_p(t)$ is a failure-free operation of a parallel system, $F_i(t)$ is a probability of a failure risk in particular elements of the system.

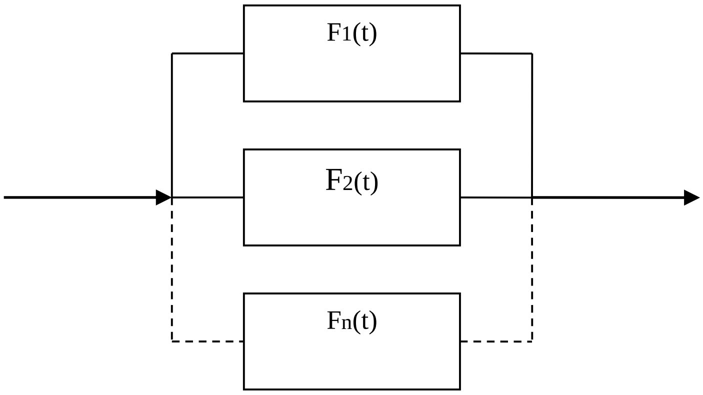

Fig.1 *System of elements with parallel arrangement of elements*

Relation of increasing reliability of the system to the number of elements in a parallel arrangement [1] is in the Fig.2.

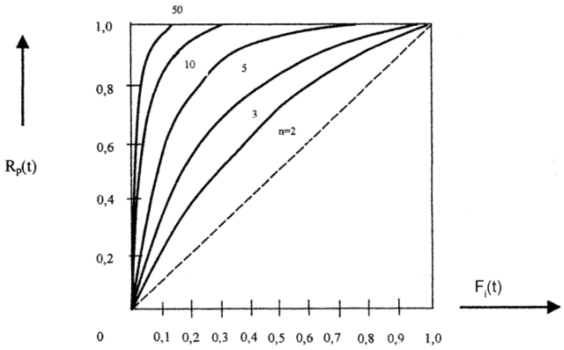

Fig2. *Relation of a probability of a parallel system failure less operation to a number of elements*

Even though a backing up increases a complexity, so its acquisition costs, in a probable deployment for special tasks in extreme climate conditions, this method has been proved as a suitable.

From a view of a special equipment crisis management the following needs have been considered:

- Access and availability, ability to pass a water obstacle; mud, mountain and forest terrain, on the road and by air.
- Mobility and equipment and systems transportation.
- Provision of electric energy.
- Provision of potable and non-potable water.
- Provision of medical and health service.

For purposes of this paper we are presenting possible ways how to provide for electric energy, potable and service water supplies and a container system to transport such equipment and systems.

2.1 Current electric energy sources used for mobile logistic assets in ISO 1C containers

Electric source units in ISO 1C containers are assigned for a production and distribution of electric energy as a backup source to provide operation of electric facilities in field conditions. They include a drive unit, a plant producing electric energy, transformer station and distribution wiring net. The power block is installed in the ISO 1C container, it is sound and thermal proof, tempering and airing is provided with embedded exhaust blowers and through orifices with closing blinds for airing. The container floor is designed as a leak-proof tub assigned to catch possible leakage of operating liquids. The container includes a sales stock for distribution wiring and power block accessories. ISO 1C container is equipped with large door with a visor and detachable panels for an easy access for a quotidian maintenance [3].

2.2 Electric sources requirements for mobile assets

One of the most important requirements to electric sources for mobile assets is applicability in a micro climate area with an N14 (STN 03 8206) climate:

- Temperature ranging from -35 °C to +55 °C,
- Relative humidity of air up to 30% at temperature of +25 °C,
- Velocity of air flow up to 20 m.s^{-1} from all directions,

Atmospheric precipitations in form of rain with intensity of 3 mm.min^{-1} falling 30° angle wise in all directions. [4]

They need to be produced so that can be connected to several kinds of distribution systems:

- TN – C, 3 + PEN, 400/231 V – the most common four-line wire distribution system,
- TN – S, 3 + PE + N, 400/231 V – distribution system used in the world,
- TT, 3 + PE + N, 400/231V – distribution system, which is not much used, however it exists in electric wiring of special equipment,
- IT, 3 + PE + N, 400/231 V – an isolated system being used mainly in special or medical equipment and in power equipment for insular power facilities. [5]

Table 2*. Electric installation parameters of some logistic container working places*

Designation and marking of a logistic container	Voltage system	Maximum power input (kW)	Output of a source itself (kW)
ISO 1C container – social	TN.S 3+N+PE 400/230V AC 50Hz	18,2	0
ISO 1C container – water tank	TN.S 1+N+PE 1x 230V, 50Hz	1,25	0
ISO 1C container – accommodation 2-bed	TN.S 3+N+PE 400/230V AC 50Hz	5,5	0
ISO 1C container – accommodation 4 bed	TN.S 3+N+PE 400/230V AC 50Hz	5,5	0
ISO 1C container – briefing folding 3- wall	TN.S 3+N+PE 400/230V AC 50Hz	7,5	0
ISO 1C container - office	TN.S 3+N+PE 400/230V AC 50Hz	6	0
ISO 1C container – refrigerator for deceased	TN.S 3+N+PE 400/230V AC 50Hz	5,1	0
ISO 1C container – refrigerator, two chamber	TN.S 3+N+PE 3x 400V, 50Hz	4,8	Combustion engine
ISO 1C container – surgery ward	TN.S 3+N+PE 400/230V AC 50Hz	9,5	

ISO 1C container – mobile workshop asset of „A”, “B” and “C” types	TN.S 3+N+PE 400/230V AC 50Hz	15	5,1

3 Conclusion

Experiences with operating the equipment in crisis and extreme conditions have proved a possibility to export and deploy machines and weaponry equipment of the SR Armed Forces into extreme climatic conditions, e.g. out of European conditions etc. With regard to development of combat activities within the theatre of operation, where a single concept in equipment is preferred in different climatic conditions, an importance of equipment adaptation to operation in various conditions is still increasing. Such adaptation is to be taken into consideration in designing equipment, as well as during logistic support of their activities as well as in planning their operation. Also published lessons learned showed a possible economical approach e.g. through a possible extension of a lifetime of some technical equipment (pressure vessels, heavy current equipment, lifting equipment) with a sustained needed operating reliability.

In terms of integration into security structures the published paper relates with a need to implement a single system of quality assessment, codification and standardization. In future it is needed to pay attention to this area with regard to a unified assessment of an operating reliability of special equipment.

References

[1] KRUŽLIAK, J. *Prevádzková spoľahlivosť, diagnostika a údržba ženijných strojov.* Liptovský Mikuláš: Vojenská akadémia Liptovský Mikuláš, 2002.
[2] BUKOVECZKÝ, J., BÍLÝ, M. *Životnosť a spoľahlivosť strojov.* Bratislava: SVŠT Bratislava, 1986.
[3] ŠÚRI, M., 2006. Solar Electricity and Prospects of its Generation in Slovakia. *Životné prostredie*. **40**(3), p. 127–132.
[4] MIKURČÍK, J. 2003. Kodifikačné minimum. *BULL-1-3*, Bulletin č. 3, VSVaP Trenčín
[5] LIPTÁK, Peter, KOPECKÝ, Ivan, GALETA, A. *Špeciálna technika. Časť Stroje a zariadenia.* Trenčín, 2005. ISBN 80-8075-053-X.
[6] ÁČ, Vladimír. 2015. *Modelovanie a počítačové simulácie systémov obnoviteľných zdrojov energie,* Čiastková správa z riešenia projektu ITMS č. 26220220083. Trenčín: TnUAD v Trenčíne
[7] KOPECKÝ, Ivan, RAKÚSOVÁ, Dana. 2014. Hybridné fotovoltické zariadenia v urbanizovaných prostrediach. *TRANSFER 2014 - 15. medzinárodná vedecká konferencia, Trenčín, 23.–24. október 2014*
[8] Dostupné z: http://www.voptrencin.sk/sk/vyvoj_vyroba_k_upr.htm
[9] Dostupné z: http://www.nuovaenergia.eu/sk/hirek/Spotreba-pitnej-vody/139/2/
[10] Dostupné z: http://www.voptrencin.sk/sk/vyvoj_vyroba_k_upr.htm

SPECIAL EQUIPMENT FROM AN OPERATION IN CRISIS SITUATIONS POINT OF VIEW, THE RESULTS ACHIEVED ON PARTICULAR EQUIPMENT

Peter LIPTÁK[1]* – Ivan KOPECKÝ[2]

[1] *Peter Lipták, Faculty of Special Technology, Alexander Dubček University of Trenčín, Pri parku 19, 911 06 Trenčín. Slovak Republic.*
[2] *Ivan Kopecký, Faculty of Special Technology, Alexander Dubček University of Trenčín, Pri parku 19, 911 06 Trenčín. Slovak Republic*
*Corresponding author E-mail address: peter.liptak@tnuni.sk

Abstract
Operation of special equipment is possible in crisis situations. It is because special equipment is designed for operation in non-standard often extreme conditions and situation. Today, everyone tries to become independent [1] with regard to persons and load transportation and number of cars increases and their comfort improves. Almost all cars are equipped with heating, ventilating and air conditioning systems [2] which make effect on environment as the cars destroy an ozone layer because of refrigerants as chlorofluorocarbon and hydro fluorocarbon used for air-conditioning and refrigeration. Other minuses of present heating, ventilating and air-conditioning systems include a significant reduction of driving range [3] of the vehicle, as a compressor is driven by the crankshaft of the engine. Maintenance and repairing cost of this system is very high.

Keywords: Peltier element, cooler, thermoelectric features, current, semiconductor

1 Introduction

This paper is seeking to overcome the demerits by replacing the existing heating, ventilating and air-conditioning system [4] by a long ago known thermoelectric couple which works on a Peltier effect. Thermo electric cooling can be considered as one of the major applications of thermoelectric modules (TEM) [5] (Fig. 1) or thermoelectric coolers (TEC). The main objective of this project is to design a cooling system installed on a conventional car ventilating fan [6]. The idea of cooling is based on Peltier effect, as when a direct current flow through TE modules it generates a heat transfer and temperature difference across the ceramic substrates causing one side of the module to be cold and the other side to be hot. The purpose of the project is to make use of the cold side to cool the ambient air to a lower temperature, so that it can be used as a personal cooler and to decrease a load of the system.

2 Generally, about a Peltier element

Cooling with a Peltier element belongs to an alternative method of cooling. A French physicist Peltier as far back as in 1834 took a think about a well-known Seeback's phenomenon. When two conductors made of different metals are connected in a close circuit and they have a different temperature, then electric current occurs in a circuit. Such connection is called a Seeback circuit. Peltier found out, that this phenomenon can be used vice-versa. If direct-current is driven into Seeback circuit, then there is a heat difference between both links. A Peltier element is based on this finding. It is formed from two semiconductor elements and a conducting bridge. Special materials (bismuth- telluride), are used as semiconductors, that have suitable thermoelectric properties, namely a low specific resistance and a low heat conductivity [7]. Copper having a low electric resistance is used for connecting links. When several elements are connected (Fig. 2), [8] so called thermo battery is created. Thermoelectric effect covers three different identified effects namely; the Seeback effect, Peltier effect and the Thomson effect. A thermoelectric device will create a voltage when there is temperature difference on each side of the device. On the other hand, when a voltage is applied to it, a temperature difference is created. The temperature difference is also known as Peltier effect. Thus TEC operates by the Peltier effect, which stimulates a difference in temperature when an electric current flows through a junction of two dissimilar materials. A good thermoelectric cooling design is achieved using a TEC, which is solid state electrically driven heat exchanger. This depends on the polarity of the applied voltage. When TEC is used for cooling, it absorbs heat from the surface to be cooled and transfers the energy by conduction to the finned or liquid heat exchanger, which ultimately dissipates the waste heat to the surrounding ambient air by means of convection. Thermoelectric generation bases on the fact that in electrical circuit consisting of different materials, connected in series, an electromotive force emerges when contacts are maintained at different temperatures. Such circuit, composed of two different materials (semiconductors of n-and p-type conductivity), is called a thermocouple or a thermo element. The device usually consists of tens or hundreds of thermo elements, connected in series.[9]

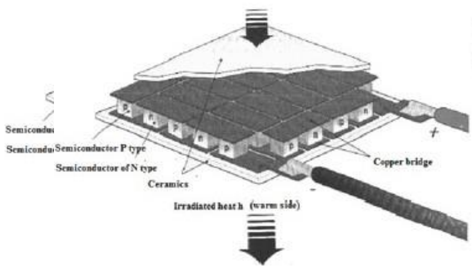

Fig. 1 Cutaway of a thermoelectric module

Fig. 2 Peltier elements composed in a cascade TE assembly with cooling capacity of 67W with 12 V nominal voltage

2.1 Temperature control with Peltier systems

Peltier systems are the temperature devices for a broad range of applications. The systems feature high heating (Fig. 3) and cooling rates (-40 °C to 200 0C) and excellent temperature accuracy. A Peltier cooler heater or thermoelectric heat pump is a solid-state active heat pump which transfers heat from one side of the device to the other, with consumption of electrical energy depending on the direction of the current [10].[can also be used as a temperature controller that either heats or cools (Fig. 4)].

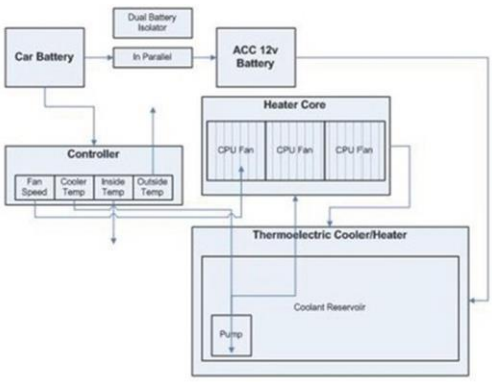

Fig. 3 Thermoelectric car air conditioner/heater

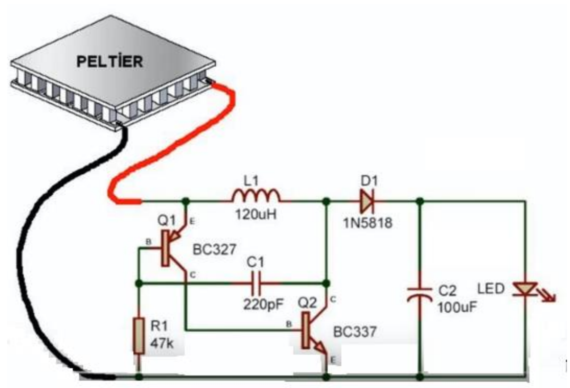

Fig. 4 Peltier- thermoelectric cooling box.

2.2 Heated/cooled thermoelectric steering wheel

Thermal comfort of vehicle occupants is an important aspect of the driving experience. Vehicle touch surfaces can gethot after being exposed to the sun. Existing steering wheels may reach temperatures that are well above the ambient temperature. Because the steering wheel may be exposed to more direct sun than other controls necessary for driving (e.g. ignition switch, shifter, brake, accelerator, seat cushions etc.), the steering wheel may be too hot to touch, thus preventing the driver from driving the vehicle until it has cooled. Traditional methods of cooling a vehicle interior space by air circulation involve opening a door or opening one or more windows. These known cooling methods require a user to be present for security reasons while waiting for the steering wheel to cool. Although it may be possible to remotely actuate a vehicle's air conditioning system in some instances, this is typically a very inefficient way to cool the steering wheel, (Fig. 5) and the steering wheel may still be too hot to touch for some time even if the cabin air temperature is comfortable. In view of the above, a need exists for an improved way to cool vehicle steering wheels. Also, if a user begins to use a steering wheel after it has been exposed to cold temperatures, the user may experience discomfort upon contact with the cold wheel. Although heated steering wheels have been developed, known heated steering wheels may suffer from various drawbacks due to limits in the amount of heat available to heat the steering wheel. There are many patented solutions dealing with a heated/cooled thermoelectric steering wheel supported with a Peltier device. A steering wheel includes a central portion connected to the steering column for rotation about an axis, and a rim extending around the central portion. A steering wheel includes a passageway extending through portions of the steering wheel. A plurality of spaced apart rings are disposed on the rim, and a plurality of n-type and p-type thermoelectric elements are located on the rings. The thermoelectric elements may comprise Peltier devices in the form of relatively thin plate-like units having generally superficial opposite surfaces, and rectangular perimeters. An electrical conductor interconnects the p-type and n-type elements in series. The steering wheel includes first and second thermal conductors thermally connected to inner and outer surfaces of the thermoelectric elements. An air circulation device moves air through the passageway to cool the rim of the steering wheel.

Fig. 5 The set-up of the thermal steering wheel. The Peltier element can be seen on the left (red circle) mounted on a heat sink.

2.3 Air-conditioning in a car

In the cars with air cooled engines there is little room for conventional air compressors and therefore we are looking for electronic means of getting cooled air into the interior and Peltier devices could be a solution. There is about 2,5 m^3 so not a lot space is needed but with ambient external summer temperatures ranging from 30 ºC to 42 ºC and a large, almost horizontal windscreen, internal temperatures can get as high as 60 ºC.

2.4 Heated mirror

Heated mirrors (Fig. 6) on vehicles keep themselves free from ice and haze the same way the defroster keeps the windshield clear. A small amount of heat is applied to the glass surface of the side mirrors. The heat evaporates moisture on the glass' surface and melts any ice that has built up. Because of blind spots behind the car, the convex mirror can make a rear view more widely. Heating function is a basic function.

Fig. 6 A heated rear mirror

2.5 Advantages of a Peltier element

- No cryogen is needed. TEC modules can work constantly for hours. It contains no pollution or rotating components, which results in no noise and vibration, long life span and easy installation.

- Very short heating-up and cooling time due to small thermal lag in TEC modules. The maximum temperature difference will be achieved within one minute under the condition of good heat dissipation in hot side and no load in cold side.

- Thermal electric cooler is a kind of current-to-energy device. By controlling the current. High precision temperature control can be achieved. Plus temperature measurement and control, it is easy to make an automatic control system with the function of remote control, program control and computer control.

2.6 Disadvantages of a Peltier element

Thermoelectric coolers are constructed based on alternating junctions between n- and p-doted semiconductors. Subjected to electrical current, the desired heat flux will be generated (Peltier effect). However, the Peltier element's capacity to cool is not infinite: the more current the Peltier controller delivers, the more Joule heat is generated. This is a parasitic heating effect that will completely cancel out the desired cooling effect above a certain threshold [11]. In practice, this means that a thermoelectric cooler driven near its maximum current rating may hardly cool at all. However, if a more advanced TEC controller with DC output is chosen the Peltier controller is working at its nominal efficiency (85° C and more) and the Peltier module is working under optimal conditions.[11]

3. Conclusions

The authors in publication summarize results of research within the „Use of renewable sources of energy in practice“ project. System of modeling and computer-aided simulation of renewable sources of energy has been proposed within this project.

Application of a system for designing of power systems in logistic containers is expected. Peltier element is nowadays used in many ways as incorporated into thermoelectric modules. The parameters obtained from the devices used in car show that reduction of power used for heating, ventilating and air-conditioning systems in a car with Peltier elements is significant, the same relates to reduction of space needed for such devices. Moreover, Peltier elements are environment friendly. Such device is easy to mount even in home conditions however the costs for such assembly are almost the same as from factory. It is very important to take the size of temperature difference into account as this feature is important for operation.

Thermoelectric system working with Peltier elements is environment friendly, compact and affordable stability control system.

Acknowledgements

The paper was completed with a support by MSM GROUP, s. r. o. , 018 41 Dubnica nad Vahom, Sturova 925/27, Slovakia as a result from common developed projects. This work was supported by the Research Agency of the Ministry of Education, Science, Research and Sport of the Slovak Republic under the contract (ITMS2014+) no. 313011W442 - CEDITEK II.

References

1. J. Stodola: 2018. - Tribology and reliability. Transport Means. - Proceedings of the Intemational Conference. Scopus
2. J. Stodola, M. Pombslci, P. Hybler: 2018.-Acceller possibilities of using accelerated electron beam for testing engine oil media - Chemicke listy
3. J. Stodola, P. Stodola: 2018 - Lecture Notes in Computer Science (including subseries Lecture Notes in Artificial intelligence and Lecture Notes in Bioinformatics).
4. J. Stodola, P. Novotny: 2017 -Virtual Engine a Tool for Tmck Reliability Increase: lOP Conference Series: Material Science and Engineering.
5. J. Stodola, J.Furch: 2017 -Risk and safety assessment of special systems. :WMSCI -21'1World Multi-Conference on Systemics, Cybernetics and Informatics, Proceedings.
6. J. Furch, J. Stodola: 2017 -Proactive maintenance example of selected part of the land motor vehicle : WMSCI-2 I" World Multi-Conference on Systemics, Cybernetics and Informatics, Proceedings.
7. P. Stodola, J. Stodola: - 2014 - Defense application of nanotechnology : Transport Means - Proceedings of the lllrnational Conference.
8. N. Luptakova, F. Peslova, P. Stodola, J. Stodola: 2015 Microstructural studies and analysis of hard zinc: Transport Means -Proceedings of the International Conference.

9. J. Balla, M. Macko, Z. Krist, S. Timar, I. Kopecky: 2017-Inserting cartridges using electrically powered ramming devices: 6th International Conference on Military Technologies.
10. J. Balla, S. Prochazka, M. Macko, S.Timar, P. Liptak: 2017-Autoloader functional diagram determination handling fixed ammunition: 6th International Conference on Military Technologies
11. https://www.meerstetter.ch/compendium/heating-and-cooling-with-a-peltier-controller

HIGH-ENERGETIC MATERIALS IN DEFENCE INDUSTRY

Peter LIPTÁK[1]* – Barnabáš KOVÁCS[2]

[1] *Peter Lipták, Faculty of Special Technology, Alexander Dubček University of Trenčín, Pri parku 19, 911 06 Trenčín. Slovak Republic.*

[2] *Ivan Kopecký, Faculty of Special Technology, Alexander Dubček University of Trenčín, Pri parku 19, 911 06 Trenčín. Slovak Republic*

*Corresponding author E-mail address: peter.liptak@tnuni.sk

Abstract

High-energetic materials involve operations with special equipment. An application of new non-traditional materials – composites and nano-materials makes this field highly up-to-date and from a research point of view it is needed to pay attention to it. The paper presents current characteristics of such materials, their classification and supposed trends of their development. Research in the field of high- energetic materials makes a mutual progress conditional on mechanical and electrical engineering, which includes special equipment. The paper also deals with issue of mutual interaction of weapon and ammunition systems containing energetic materials. Work with high-energetic materials is not only a part of work for defence industry as well as a part of work in crisis management, mining, building and other parts of the life of a society.

Keywords: High-energetic materials, explosives, special equipment, nano-materials, composites, crisis management.

1 Introduction

The explosives form a significant part of many kinds of ammunition. The explosives are substances able to produce an explosive transformation (fulminating compounds, traskaviny, high explosives -trhaviny, propellants, streliviny, pyrotechnical composites) [1].

Therefore the ammunition includes projectiles of various kinds, effective heads of rocket systems, hand grenades, bombs, engineering mines, and in accordance with their assignement, they contain explosives or determine their composition [2].

2 High-energetic materials

High-energetic materials are substances able to develop a extremely rapid exothermic reaction associated with development of a huge volume of gases having high temperature [1].

A reaction is launched through an initiation by a mechanical, thermic (thermal) electric incentive or by a blasting wave. Composite explosives may contain substances of an explosive nature (explosives), auxiliary substances adjusting needed features of a composite explosive, as well as substances, that are not explosive. A part of a composite explosive is a substance of a non-explosive nature, as a rule a suitable fuel and an oxidizer, providing a chemical reaction with an oxygen needed for burning, as an amount of an oxygen delivered from an ambient atmosphere is not sufficient for combustion of the compound in a sufficient short time period[3], [4].

The explosives are classified among fuels and sometimes they are designated as energetic materials. The term of an energetic material is a wider and it includes for example components of liquid rocket fuels as well.

By a practical application the high-energetic materials are divided into:

a) **Fulminating compositions** – are easily inflammable explosives, which usually serve to an initiation of high explosives or propellants. They are featured in a transition from an explosive burning into a detonation. They are present at a practical application only in a non-significant amount, e.g. a fulminating composition in a blasting cap - or in an ignition cap e.t.c. The most common types of fulminating compositions are various azides of heavy metals as lead, silver or quicksilver or other substances. Mercuric fulminate is widespread (a popular fulminating quicksilver).

b) **High explosives** – are explosives, which are relatively sparsely sensitive to external influences and on contrary when initiated they can detonate with a high detonation speed. As a rule they are applied at blasting operations in mines, quarries, in tunnel excavations, demolitions and in charges of military ammunition. The most widely applied fulminating compositions include pentrite, hexogen, TNT and their compounds, then dynamites and a large amount of industrial explosives having different composition. A lot of compound explosives, military ones, but first of all industrial ones, use ammonium nitrate as their basic element. A typical explosive transformation of high explosives is a detonation. In a poor initiation or in a flame ignition many high explosives do not detonate, but they get into an explosive combustion (in an enclosed space), or it burns down as a normal organic combustible (in an open air). The transition of an high explosive from detonation into explosive burning is highly undesirable phenomenon, as a destruction usually occurs, but in a lesser extent than it was planned.

c) **Propellants** – are used as a propellant charge for cartridge cases of fire arms for military, sport and hunting purposes. They are aiming to provide a projectile with the highest mechanical acceleration, also to force a projectile out from a weapon barrel tube with the highest or required velocity through a controlled development of huge amount of hot gases. A black gun-powder and propellants based on nitrocellulose (projectile cotton wool) is an example. Propellants include also rigid fuels. A typical transformation of explosives is an explosive combustion. Velocity of combustion in a propellant varies and it depends on pressure and temperature, at which an explosive combustion takes place. Velocity of explosive combustion increases with an increasing pressure and temperature. In an extreme case, the explosive combustion of the propellant gets down to a detonation –however such behaviour is extremely unwanted, as it results in an accident (it means fragmentation, destruction) of the weapon or a rocket engine. Propellants can be brought directly to a detonation through a sufficiently strong impulse and then they behave as high explosives.

d) **Pyrotechnical composites** – are mixtures of flammables, oxidizers and other auxilliary substances, creating respective pyrotechnical effect. They can be also illuminating and signal compounds, tracer compounds, ignition compounds, flashing compounds, acoustic compounds (whistling sound) and many others. A typical explosive transformation is almost wholly explosive combustion. Sometimes pyrotechnical composites are not included in explosives.

The explosives are classified in high explosives and fulminating compositions due to their practical purpose, but also by their features – a typical high explosive can not be easily activated by a simple impulse; the fulminating compositions in amounts, that are used, are extremely dangerous. While a production capability of a line producing tritole can reach tens of tonnes, a daily capacity of a line producing fulminating compounds represents only tens of kilograms of a fulminating quicksilver or units of kilograms of lead azide or other fulminating compounds [5], [6].

<u>The propellants are divided by their specification in :</u>

- Black gun- powders and pyrotechnical compounds, assigned mainly for ammunition laboration, i.e. activators, tracers;
- Smokeless powders and combustible pastes are assigned mainly for barrel tube weapons;
- Rigid fuels, mainly assigned for rockets

<u>The smokeless powders are divided by their typical elements into:</u>

- Single-compound (nitrocelullose) smokeless powders, a main component is nitrocelullose („nc‟)
- Double-compound (nitroglycerine) smokeless powders, main components are nitrocelullose, plastified with nitroesters (nitroglycerine „ng‟) and (dietylenglycol-dinitrate „dg‟)
- Three-compound nitramine smokeless powders, containing in addition to nitroglycerine and dietylenglycoldinitrate as well crystalline nitramines (hexogen-RDX)
- Three-compound nitroguanidine („nq‟) smokeless powders (for example for 155 mm ammunition)
- Special types of smokeless powders, assigned for laboration of igniters (designation BENITE, or CBI- porous nitrocelullose powder)
- Combustible bodies used as a propellant charge for large caliber munition)
- Spheric powders with a low content of nitrocelullose (about 10%) produced with a special technology [7].

3 Powder charge

Powder charge is made up from powder grains of various shapes (balls, straps, slices etc.). Powder grains are made of powder paste, which is mostly of diglycol, nitroglycerine or nitrocelullose [7].

Fig. 1 Black gun-powder [7]

Black powder usually means a compound of potassium nitrate, sulphur and charcoal. Smokeless powders, nitrocellulose ones, but also nitroglycerine ones, contain some inert substances, that generate smoke as well when fired, that might reveal a firing position during the day. Smokeless powder can be also a mechanical mixture of ammonium saltpeter and charcoal.

From the end of the XVIII century it has been produced having almost the same composition, namely:

75% - potassium nitrate (KNO_3);
15% - charcoal (C);
10% - sulphur (S) [7] .

First, these three compounds are ground, then are mechanically mixed so that they form a homogeneous mixture, that is called black gun-powder after having been pressed in a shape of pressed grains. Composition is changed depending on the application of the powder in practice.

There are powders, where dinitroglycol or nitrotoluene is used during their production instead of nitroglycerine and therefore these powders can not be classified into no class, therefore they form a separate group.

The most typical feature of the powder is a nature of its combustion process and conditions, at which this powder burns down depending on a powder geometry. All powders form mechanical compounds, that do not burn fully regularly and when the powders with a low mass burn down, they are not subject to any combustion rule. All powders of colloid nature (i.e. gelatinate), based on pyroxyline (nitrocellulose) burn regularly, by a combustion rule in parallel layers (geometrical rule). In case, we will consider physical –and- chemical properties of the powder as dividing criteria, the powders can be classified in two main groups:

1. powders – mechanical compounds;
2. powders – colloid compounds (gelatinate).

Mechanical compounds fall then in:

1. Black powders, composed of potassium nitrate, sulphur and charcoal, containing about 75% potassium nitrate , 10% sulphur and 15% charcoal. So the powders prismatic, coarse-grained, artillery ones, rifle, hunting, blasting and timing ones.

2. Ammonia-potassium nitrate powders, containing about 90% of ammonia-potassium nitrate and 10% of charcoal.
3. Other kinds of powders , that are similar to a black gun-powder by their composition, are called powder of colloid type based on nitrocellulose and based on nitroglycerine. Those based on nitrocellulose are gained through gelatinization of a nitrocellulose by means of volatile solution, the others are obtained through gelatinization of a nitrocellulose by means of nitroglycerine. In accordance with a kind of a solution used in a preparation of the powder, they are divided in:

1. Powders with a volatile solvent;
2. Powders with a little volatile solvent;
3. Powders with a non-volatile solvent.

Powders with a volatile solvent contain nitrocellulose and rests of alcohol-and-ether compound, which was a solvent itself, in addition to difenilamine and centralite, being stabilizers, plus admixtures, for example to damp a flame and others. By a purpose and a way of application these powders are classified in:

1. Rifle powders;
2. Artillery powders;
3. Powders for special purposes (burning quickly, flameless, powders with an increased performance etc.).

Powders with a little volatile solvent are divided by their composition in ballistites and cordites. These powders contain nitrocellulose, nitro-glycerine, and centralite, acetone, moisture (humidity), vaseline and other admixtures. Difference between ballistites and cordites is in a fact, that ballistites contain no volatile solvents and nitrocellulose with a mean content of nitrogen is used for their production. Cordites contain rests of volatile solvents and nitrocellulose with a high content of nitrogen (piroxiline) is used for their production. This group of powder includes powders with a dinitroglycol solvent.

Powders with non-volatile solvent are relatively new and meanwhile they are rarely used in practice. These powders contain nitrocellulose (pyroxiline), rigid solvent (trotyl, dinitrotoulene, and dinitroanisol), a stabilizer, some humidity and eventually a small rate of additions (max 2%).

3.1 Smokeless powder

Smokeless powders are explosives, creating hot fumes delivering a movement through their defined explosive combustions to a projectile in a barrel tube when fired. The required inner ballistic features of a smokeless powder are determined by its chemical composition, by features of an applied nitrocellulose, by a way of processing, by a shape and size of a grain, or by geometrical parameters of a grain.

Smokeless powder is used as a driving charge for all kinds of cartridges for barrel-tube arms, from cartridge cases of small shooting arms, through cartridges of medium calibres assigned for canons, up to cartridges for large-caliber howitzers and howitzer systems.

Smokeless powders are compounds based on nitrocellulose, where additional substances are admixed to polymer matrices so that they adjust resulting features, or substances improving the way of their processing. The features of an applied nitrocellulose make a radical effect on mechanical as well as ballistic features of a resulting smokeless powder. Important features of a nitrocellulose are mainly content of nitrogen, and molecular mass of this polymere. Nitroglycerine, diethylenglycoldinitrate, diethanolnitramine dinitrate, pure 2,4-dinitrotoluen, a technical dinitrotoluen (compound of 2,4- and 2,6- isomers), or a so-called liquid trotyl (compound of dinitrotoluen and trinitrotoluen isomers) are used as explosive gelatinators of a nitrocellulose, softening a nitrocellulose matrix and adjusting its explosion heat. Also non-explosive gelatinators (dibutylftalate, or Centralite I) are used for softening the nitrocellulose matrix. Some crystalline explosive fillers (e.g. nitroguanidine, reducing a powder errosiveness) can be added into a softened nitrocellulose matrix. Some organic stabilizers(difenylamine, Centralite I a Centralite II) are added into a compound aiming to stabilize a smokeless powder, chemically binding nitrogen dioxide on themselves, having been generated through a decay of nitrocellulose and other contained organid nitrates. Substances as Centralite I, technical dinitrotoluen, dibutylphtalate, or camphor are used in smokeless powders aiming to slow down a combustion, mainly on surface layers of the powder (a function of surface flegmatizers). Some organic substances based on waxes, vaselines or a transformer oil are added into a powder to improve a compressibility. Anorganic substances play a role of combustion catalyzers in smokeless powders (oxide and lead carbonate, calcium carbonate, tin dioxide), stabilizers (magnesium oxide, calcium carbonate), flame damper (potassium sulphate), substances increasing a grain porosity (natrium sulphate, potassium nitrate), substances improving a powder compressibility (zincous sulphate) and substances improving working properties and a specific mass of the powder (graphite).

Smokeless powders are produced in form of grains of various shapes – slices, rollers, roundels, balls, rings, tubes with one or more (max. seven) lengthwise orifices etc.

Designation of smokeless powders of a Czech production, having been commissioned within the Army of the Czech Republic, as well as in the Armed Forces of the Slovak Republic includes information about a chemical composition of the powder, its geometric shape, dimensions, some features or admixtures, a manufacturer, series, and a year of production.

Smokeless powders are classified by their chemical composition in single-compound nitrocellulose powders having been with no content of explosive softeners using volatile solvents, designated with an abbreviation (Nc). Double-compound nitro-glycerine powders containing nitro-glycerine, designated with an abbreviation (Ng). Double-compound diglycol powders containing diethylenglycoldinitrate, designated with an abbreviation (Dg) and a triple-compound gudole ones containing nitro guanidine, designated with an abbreviation (Gu, or NQ).

The designation following an abbreviation of a chemical composition states a shape of a smokeless powder grain, which is really a little bit smaller, as volatile substances of a solvent release from powder resulting from storage. If the powder has a special designation (e.g. Nc dp C1, Ng sp sample 43), its dimensions and other data are not provided.

Other data include powder designation following its characteristic size, as numerical or written data indicating its features (eg. Explosion heat, or some additives). In case that some powder is produced by license documentation sometimes there is a designation of original powder in brackets (so called equivalent).

The last data in a powder designation is a manufacturer designation and designation of a production series. Manufacturer designation is stated by a code, consisting of three letter designation, or a mark (eg. S&B). Powder series is designated with a serial number, which is the last two figures of the production year.

Homogenized powders are designated with a serial number of a homogenized series, described with Roman numerals and slashed following a year of homogenization. This designation is written or following a designation of an original series, or it is stated separately. Homogenized powder can be designated with a serial number of a homogenized series with Arab numerals and slashed with two numerals of the year of homogenization – it is additional option for designation. Such designation was done for smokeless powders having been homogenized in a laboration works, in such a case, it consists of three numerals always starting with a digit 5. Designation R (retour) after a serial number means, that some part or amount was used from a previous production (series) or from remade older series of the powder [8], [9].

For example a designation Nc tp 3x1,25 / 3,5-F1 WXH 501/80 means a nitrocellulose tube-shape powder with a matrix dimension: 3,0 mm (a grain diameter), 1,25 mm (thickness of a grain wall), 3,5 mm (grain length), surface flegmatized (with camphor- terpenoid), manufacturer WXH, series 501, year of homogenization 1980, allows determining basic parameters without material sheets.

Smokeless powders and a homogenous TPH of a Czech production can be designated also with commercial designation of the manufacturer (Explosia Pardubice-Semtín a.s.), with a starting letter S (a single-compound, nitrocellulose), or with a D letter (double-compound, nitro-glycerine or diglycole or multi-compound ones) and a serial number with three-digit designation (in an older version), or put to five-letter designation (in a newer version), i.e. a serial number (e.g. S 020). The mentioned three-numeral does not express a particular value of features of a smokeless powder, however as a rule the velocity of powder combustion decreases with an increasing number (it is only an orientation aid). The last two digits in a five-digit code (e.g. 02 in a designation D 100-02) represents a modification of a powder mass (e.g. D 100), assigned for a particular customer or an application[8], [9].

The smokeless powders together with homogenous rigid fuels are the least stable military explosives; such instability is caused by a chemical decay (denitriding) of a nitrocellulose and liquid nitroesthers (nitroglycerine, diethylenglycoldinitrate). Whereby nitrogen dioxide is released (dioxide nitrogen and nitrate) and heat, such chemical decomposition takes place at a significant velocity at a normal temperature and therefore if a contact with a nitrocellulose is not prevented through a rising dioxide nitrogen, so a nitrocellulose decay takes place. That is why smokeless powder contains organic stabilizers (diphenylamine, Centralite I, or Centralite II), binding dioxide nitrogen on itself and in such a way it prevents their contacting with nitrocellulose (my research relates with this problem, through which I want to demonstrate a decrease of stabilisers in a long-term storage, through an artificial ageing, as in our ammunition dumps there is ammunition, which is older than 15 years, even older than 20 years). From original stabilisers some nitroso- and nitro- derivates come into being (e.g. N-nitrosodiphenylamine, 2-nitrodiphenylamine, 4-nitrodiphenylamine, 2,4-dinitrodiphenylamine up to hexanitrodiphenylamine rise from diphenylamine). If stabilization efficiency of stabilisers is exhausted then a smokeless powder becomes instable and its auto-ignition may occur.

Decay process of a powder is backed up with:

1. humidity;
2. solar radiation;
3. substances of acid or alkaline nature.

Ageing process also reduces a molecular mass of a nitrocellulose and a content of nitrogen in it that is directly reflected in mechanical features of smokeless powders. (decrease of a tensile strength, trend to a fragmentation due to ignition pressure), even an inner ballistic capacity decreases (i.e. irregular burning, pressure pulses, an intense increase of pressure during combustion of powder when fired), that may result in affecting an outer ballistics of a projectile, or up to a degradation of a weapon during firing, or shots. The inner ballistic features of smokeless powder are significantly effected by a physical instability becoming evident e.g. through a decreasing content of volatile solvents in nitrocellulose powders, through an absorption or releasing humidity, or even a migration of gelatinizators of crystalline elements on a surface of a grain itself or into a powder wrap page (e.g. a paper cartridge case) etc. The migration of nitro-glycerine itself to the grain surface reduces a powder handling safety. A specific characteristics for an advanced decay of a powder is an occurrence of stains, bubble and cracks on a surface of the grains, the powder adheres and changes its shape and becomes tender and falls apart. The last stage of powder decay is releasing of brown smokes of dioxide nitrogen [8], [9].

In explosive testing it is needed to pay attention to a stability of smokeless powders, as their instability can result in extreme cases in an accident of a degradation of weapon systems and explosion in ammunition dumps.

Rise of instability can be detected for smokeless powders through determining their content of volatile substances and their humidity, by a visual control, by determining a content of stabilisers and other extractable elements of the powder through HPLC (High Pressure Liquid Chromatography), determining a period, when an auto-catalytic decay had started, through determining a volume of released decayed gases and through determining inner ballistic features of the powder. Selected parameters need to be monitored also after an artificial ageing process.

4 Conclusion

High-energetic materials are substances, which pertain to an area of ammunition application by their nature. It is necessary to obtain knowledge relating their parameters in their practical application to get their better characteristics and understanding. For that reason, the studies, or issues need to be completed and respective consequences to be drawn. The knowledge should be involved in various regulations and technical procedures and standards in production, storage and servicing of special assignment products, for example in ammunition production.

References

1. Tišunin V.: Krátky kurs prachů. Preložil pplk. Horák VTA v Brne
2. Boldirev A: Kratkij kurs technologii porocha, vydání z roku 1932
3. Constantine R: Barel Vibrations, Ladder Test to develop Loads, Bayefield USA 2003
4. Brebera S: Vojenské trhaviny a technológie výroby trhavinových náloží, Uč. Texty Univerzita Pardubice – KTTV 2001
5. Lehký L: Technológie hnacích hmot, Uč. Texty – Univerzita Pardubice – KTTV 2001
6. Zeman S: Technologie energetických materiálu I. Pardubice, 2007.ISBN978-80-7194-939-8. Texty přednášek z predmetu Technologie základních výbušnin. Univerzita Pardubice.

7. Lehký L: Technologie hnacích hmot: Teorie a technologie výbušin. Pardubice, 2005. ISBN 978-80- 7194-901-1. Licenční studium. Univerzita Pardubice.
8. Kolektív autorov, Zborník radova, XXI simpozijum a explozivnim materilajama, Jugoslovensky komolet za explozivne materije, TARA 2001
9. Zukas, A.J., Walters W.P. (Ed.): Explosive Effects and Applications, Springer-Verlag, N.Y. 1998